Neuron-Aware Active Few-Shot Learning for LLMs

Anonymous ACL submission

Abstract

Active Few-Shot Learning (AFSL) adapts LLMs to specialized domains by identifying the most valuable unlabeled samples for annotation and use as few-shot demonstrations, effectively reducing human annotation costs while promoting high performance. However, existing methods typically rely on output-level signals for the sample identification, such as predictive entropy or semantic similarities with test-time data based on external embeddings, which often overlook models' internal dynamics which could pinpoint specific knowledge gaps. To bridge this gap, we propose **NEUFS**, a **Neu**ron-Aware Active **F**ew-**S**hot Learning framework that shifts the selection paradigm from output-level proxies to models' internal dynamics. NEUFS utilizes neuron activation patterns to represent sample directly, and includes a dual-criteria selection strategy that: (1) ensures few-shot sample diversity with neuron patterns for broader example coverage, while (2) prioritizing on identifying informative and challenging few-shot samples LLMs tend to hallucinate by quantifying *neuron consensus*. Experiments on three datasets demonstrate that NEUFS excels in both reasoning and text classification tasks, outperforming existing AFSL baselines. Ablation studies further highlight that internal neuron activations provide a more principled and effective selection signal than external embeddings, validating the superiority of the proposed NEUFS.

1 Introduction

While recent advances in LLMs have greatly improved general tasks like text classification, these models often fail to perform well out-of-the-box in specialized domains such as education, medicine, or law. Adapting off-the-shelf models to these expert fields is typically made difficult by the scarcity of data and the computational costs required for fine-tuning. To adapt LLMs for specific downstream tasks, few-shot in-context learning (ICL) has emerged as a popular training-free adaptation strategy. By providing examples within the query context, ICL has demonstrated promising performance in practical applications (Brown et al., 2020). The selection of few-shot has been identified as a critical factor for downstream task performance (Min et al., 2022).

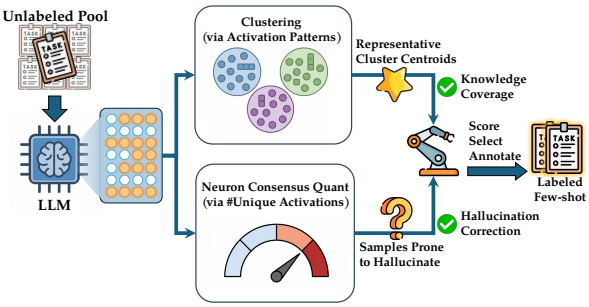

Figure 1: Neuron-Aware AFSL, which identifies informative and diverse few-shot samples for annotation. By leveraging activation patterns, NEUFS ensures broad knowledge coverage through activation pattern-based clustering while targeting informative, hallucination-prone samples via neuron consensus quantification.

Existing work on few-shot example selection typically assumes access to a large annotated dataset, where retrieving examples most similar to the test data at inference time yields the best performance (Yu et al., 2023a; Margatina et al., 2023). However, constructing large annotated datasets for test-time retrieval is oftentimes impractical, especially for specialized domains that require expensive expert-level annotations. Consequently, exploration of few-shot selection strategies under unlabeled data settings remains limited. Recent work has begun to address this gap by introducing active learning (AL) into few-shot ICL, i.e Active Few-Shot Learning (AFSL) (Ahmadnia et al., 2025).

AFSL extends traditional AL techniques to the few-shot paradigm, selecting the samples from a large unlabeled pool that are most likely to yield strong test-time performance, to be annotated as ICL demonstrations, providing a promising solu-

tion for reducing annotation costs while maintaining performance (Xia et al., 2025; Ahmadnia et al., 2025). AFSL methods largely follow the intuitions of mainstream AL approaches, which either prioritize highly uncertain samples to select informative samples (Meng et al., 2019; Gal et al., 2017), ensure semantic diversity in the selected set (Yuan et al., 2020), or consider both (Guo et al., 2024; Yu et al., 2023b; Hongjin et al., 2022).

For informativeness, uncertainty measurement using entropy is commonly adopted. However, in the context of LLMs, it suffers from overconfidence and hallucination issues (Huang et al., 2025), which LLMs can be confidently wrong. Moreover, the misaligned objectives of next token prediction and knowledge assessment further compound these limitations, meaning token predictive entropy cannot fully represent LLMs' intrinsic knowledge dynamics (Kuhn et al., 2023). For diversity, previous work relies on applying an external model to extract sample representations, then select samples through clustering (Ahmadnia et al., 2025) or KNN algorithms (Hongjin et al., 2022). The strong assumption of semantic-knowledge equivalence causes the sub-optimal performance, that is, semantically similar samples can incentivize completely different knowledge when performing a specific task. Overall, most methods rely on output-level model signals (Guo et al., 2024; Ahmadnia et al., 2025).

To address these concerns, we shift from output-level signal toward internal model dynamics for AFSL. Recent work indicates that neuron activation patterns in the Feed-Forward Networks (FFNs) of LLMs can link to multiple concrete knowledge concepts (Gao et al., 2024). Moreover, neuron activations could indicate potential hallucinations and model utility (Chen et al., 2025; Cao et al., 2025). Specifically, higher neuron consensus corresponds to fewer hallucinations. Thus, utilizing these internal dynamics provides a more robust and principled signal for AFSL by directly revealing the underlying activation patterns associated with the LLMs' internal knowledge and potential hallucinations.

To this end, we introduce **NEUFS**, a **Neuron-Aware Active Few-Shot Learning** framework that shifts the selection paradigm from output-level signals to internal model dynamics. As illustrated in Figure 1, NEUFS ensures broad knowledge-level coverage by diversifying neuron activation patterns via clustering and facilitates hallucination mitigation by leveraging neuron consensus as a uncertainty proxy. This strategy allows the selection to prioritize samples that trigger unique knowledge circuits or those where the LLM is prone to hallucinates. Extensive experiments on four models across three tasks ranging from complex reasoning to text classification demonstrate our method's strong generalizability and competitive 1^{st} or 2^{nd}-ranking performance. Codes have been released[1].

2 Related Work

2.1 Active Learning

AL aims at reducing annotation costs by selectively annotating the most valuable samples from a large pool of unlabeled data for model learning, while maximizing LLMs' performances (Cohn et al., 1994). For AL, previous work have proposed to select samples based on uncertainty (Meng et al., 2019; Gal et al., 2017), semantic diversity (Yuan et al., 2020), or jointly considers both (Guo et al., 2024; Yu et al., 2023b; Hongjin et al., 2022). As AL aligns with the nature of few-shot learning, where demonstrations are crucial as well, Margatina et al. (2023) analyzed AL in the few-shot setting, discovering that similarity between the testing query to the demonstrations is the key factor in few-shot selections, which aligns with their strong performances, such as TypiClust (Hacohen et al., 2022).

However, most existing methods remain data-centric or rely on output-level signals, such as predictive entropy. In the context of LLMs, it suffers from overconfidence and hallucination issues (Huang et al., 2025), and the misaligned objectives of language modeling and knowledge assessment further compound these limitations, meaning token predictive entropy cannot fully represent LLMs' intrinsic knowledge dynamics (Kuhn et al., 2023). Though gradient-based methods are being proposed recently (Jung et al., 2025), they often run with the ground truth label and require a significant computational resource overhead. In contrast, our approach is model-centric. We bypass these lossy external proxies and output-level signals, and select demonstrations based directly on internal neuron activation patterns, ensuring that the selected samples align with the model's cognitive processing.

2.2 Neuron Analysis

Techniques for analyzing internal model states have evolved from linear probing (Nostalgebraist, 2020) to sophisticated mechanistic interpretations (Gao et al., 2024). Early work utilized the Logit

[1]Anonymous Link Masked

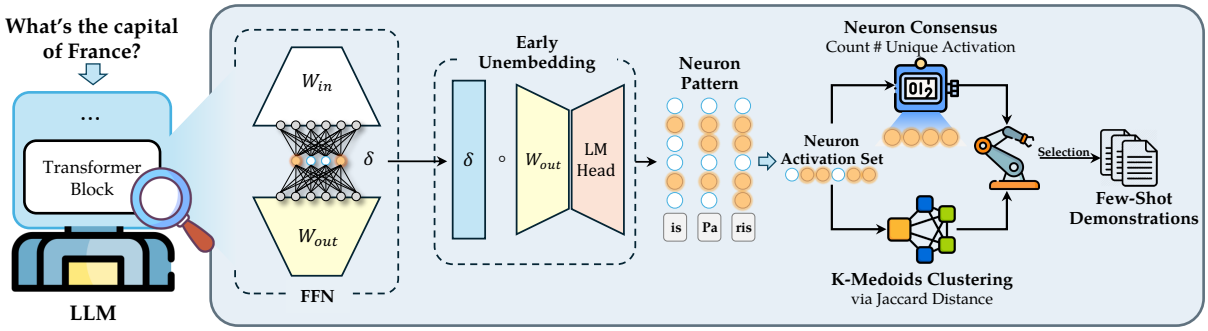

Figure 2: Overview of the proposed NEUFS. For each candidate, we extract the activation values from the FFN in each layer transformer during answer generation. Then we calculate the contribution score of each neuron via early unembedding, thereby identifying the activated neurons. Next, we perform Neuron Consensus Quantification by counting unique activations and K-Medoids Clustering via Jaccard distance for sample scoring and selection.

Lens (Nostalgebraist, 2020) and Tuned Lens (Belrose et al., 2023) to map intermediate activation values in FFNs to vocabulary space. Recently, Sparse Autoencoders (SAEs) have achieved promising results in resolving neuron superposition and disentangling polysemantic features (Gao et al., 2024).

Beyond feature extraction, recent studies have established a direct link between internal activation patterns and model reliability. Chen et al. (2025) showed that internal neuron consensus, which is defined as the number of activated neurons across related neurons, serves as a strong indicator of hallucination, where higher consensus correlates with factual correctness. Similarly, Cao et al. (2025) introduced mechanism-interpretable metrics to evaluate model utility beyond surface-level performance, further validating the significance of internal signals. However, while these insights link internal states to generation quality, their application to data selection remains underexplored. Our work bridges this gap by proposing a new paradigm which leverages these internal activation signals for AFSL.

3 Methodology

NEUFS operates as a pipeline for AFSL, instead of relying output-level signals, we proposed to shift the selection paradigm toward internal model dynamics by utilizing neuron activation patterns to represent samples directly. As illustrated in Figure 2, the framework consists of three sequential stages designed to capture the LLM's internal neuron states and uncertainty. First, we retrieve the raw activation values from the FFNs across all transformer layers for each candidate sample. Second, we employ **Neuron Activation Identification** via early unembedding to filter for neurons that contribute significantly to the model's final prediction. Afterwards, we execute **Neuron-Aware Active Few-Shot Selection**, which integrates *Neuron-Aware Sample Diversification* with *Neuron Consensus Quantification*. This combination prioritizes samples that trigger unique knowledge circuits that LLM tends to hallucinate, while ensuring the selected samples remain representative and diverse.

3.1 Neuron Activation Identification

To capture the internal dynamics of LLMs, we focus on neuron activations in FFNs, which are widely regarded as the key-value memories storing factual knowledge (Geva et al., 2021). However, neuron activations does not strictly imply task relevance, neurons often exhibit polysemanticity or encode noise. To filter for neurons that genuinely support the model's internal reasoning process, we employ *Early Unembedding* (Chen et al., 2025).

Formally, consider an LLM with L layers. For an input sequence x, let $\mathbf{h}^l$ denote the input hidden state to the FFN at the l-th layer. The FFN consists of an up-projection matrix $\mathbf{W}_{in}^l \in \mathbb{R}^{d \times d_{ff}}$, a non-linear activation function $\sigma(\cdot)$, and a down-projection matrix $\mathbf{W}_{out}^l \in \mathbb{R}^{d_{ff} \times d}$, where d_{ff} is the intermediate dimension of the FFN and d represents the dimension of hidden states. The neuron activation values $\mathbf{k}^l \in \mathbb{R}^{d_{ff}}$ are computed as:

$$\mathbf{k}^l = \sigma(\mathbf{h}^l \mathbf{W}_{in}^l),$$

where k^l represents the activation value at the transformer layer l, and k_i^l is the i-th activation value.

While the activation value k_i^l indicates how a neuron is activated, it does not directly reveal the semantic concept it promotes. To bridge the gap between internal states and output vocabulary, we

analyze each neuron's contribution to the final prediction through the unembedding matrix in the LM head $\mathbf{E}_u \in \mathbb{R}^{d\times V}$, where V is the vocabulary size, to decode neuron activations into a distribution over the vocabulary.

Let $\hat{y}$ be the prediction token generated by the model for the input x. The contribution score $S^l_{\hat{y},i}$ of the i-th neuron in layer l to the predicted token $\hat{y}$ is calculated by projecting its corresponding output vector directly into the vocabulary space:

$$S^l_{\hat{y},i} = k^l_i \cdot (\mathbf{w}^l_{out,i} \cdot \mathbf{e}_{\hat{y}}),$$

where $\mathbf{w}^l_{out,i}$ is the i-th row of the down-projection matrix $\mathbf{W}_{out}$, and $\mathbf{e}_{\hat{y}}$ is the embedding vector corresponding to the predicted token $\hat{y}$ in $\mathbf{E}_u$.

This score $S^l_{\hat{y},i}$ explicitly quantifies how much neuron i in layer l contributes to the predicted token $\hat{y}$. Following Chen et al. (2025), we identify the set of *valid* activated neurons $\mathcal{N}_{act}$ by filtering out those with contribution scores below the threshold. Specifically, the threshold is defined through a topk process, by selecting the highest k neuron activations across all activations in the FFN layers. For a given threshold η, the activated neuron set is defined as the collection of neurons whose contribution scores exceed this value:

$$\mathcal{N}(x,\hat{y}) = \left\{(i,l) \mid S^l_{\hat{y},i} > \eta\right\},$$
$$\mathcal{N}_{act}(x) = \mathcal{N}(x,y_0) \cup ... \cup \mathcal{N}(x,y_t),$$

where y_t is the t-th token in the predicted sequence, and η is dynamically determined to retain the top-k most contributive neurons globally. Specifically, for computational efficiency, we employ a two-stage filtering process. We first retrieve the top-n[2] neurons from each layer based on raw activation to form a neuron pool. From this pool, we rank all neurons by their contribution scores and select the top-k neurons as the activated neurons, which implicitly sets η to the contribution score of the k-th ranked neuron. This resulting set $\mathcal{N}_{\text{act}}$ serves as a sparse representation of the knowledge invoked by the LLM to process sample x, which forms the basis for subsequent selection.

3.2 Neuron-Aware Active Few-Shot Selection

After identified the valid activated neurons for each candidate, we apply them to the selection process. The core objective of NEUFS is to select a set of few-shot samples that are both *representative* of the underlying task knowledge and *informative* for correcting potential model hallucinations. As shown in Figure 2, our pipeline integrates two distinct signals derived from the internal model dynamics: neuron activation patterns and neuron consensus.

Specifically, we first perform clustering based on the identified neuron sets to ensure the diversity of the selected examples. Simultaneously, we quantify the neuron consensus for each sample by counting the unique activated neurons during the generation process, serving as a proxy for hallucination risk. Finally, we employ a dual-criteria scoring that balances these two metrics to rank and select the optimal sample from each cluster.

Neuron-Aware Sample Diversification To ensure the selected demonstrations cover diverse semantic and knowledge patterns, we group the unlabeled samples based on their internal activation patterns. Unlike methods that rely on external embeddings, we utilize the sparse set of activated neurons $\mathcal{N}_{act}(x)$ as the sample representation. Given that $\mathcal{N}_{act}(x)$ is a set of discrete indices (layer, neuron), we employ the Jaccard similarity to measure the similarity between two samples x_i and x_j:

$$D_J(x_i,x_j) = \frac{|\mathcal{N}_{act}(x_i) \cap \mathcal{N}_{act}(x_j)|}{|\mathcal{N}_{act}(x_i) \cup \mathcal{N}_{act}(x_j)|}, \quad (1)$$

We then apply the K-Medoids algorithm (Kaufman, 1990) to partition the candidate pool into C clusters, where C corresponds to the target number of shots in few-shot experiments.

Neuron Consensus Quantification While diversification ensures coverage, it does not account for the quality or difficulty of the samples. Drawing on findings that internal neuron activation patterns correlate strongly with model hallucinations (Chen et al., 2025), we introduce *Neuron Consensus* as a metric for selecting informative and difficult samples. Previous work suggests that higher neuron consensus, where a smaller number of unique neurons are activated during the generation process, corresponds to fewer hallucinations. Conversely, samples with lower consensus indicate scenarios where the model's internal knowledge is sparse or conflicted, making them prone to hallucination.

For AFSL, these low-consensus samples are the most valuable as demonstration with human annotation guidance. We quantify the neuron consensus $Q(x)$ simply as the count of unique valid activations identified in the early unembedding step, a

[2] n is set to 2000 for all experiments.

higher value means lower consensus:

$$Q(x) = |\mathcal{N}_{act}(x)|, \quad (2)$$

Our strategy prioritizes samples with higher $Q(x)$, aiming to retrieve samples that trigger more unique circuits which the LLMs tend to hallucinate.

3.3 Sample Scoring and Selection

To further select the final demonstrations from each cluster, we design a dual-criteria scoring mechanism that integrates both representativeness (proximity to the cluster center) and informativeness (low neuron consensus). For each cluster $\mathcal{C}_i$ with medoid μ_i, we evaluate every sample $x \in \mathcal{C}_i$. First, we normalize the distance and consensus metrics within the cluster to ensure comparable scales. Let $\tilde{D}_J(x, \mu_i)$ be the min-max normalized Jaccard distance to the medoid, and $\tilde{Q}(x)$ be the min-max normalized number of unique activated neurons.

We define the final selection score $Score(x)$ as a weighted combination of these normalized metrics:

$$Score(x) = \tau \cdot \tilde{Q}(x) + (1 - \tau) \cdot \tilde{D}_J(x, \mu_i). \quad (3)$$

where $\tau \in [0, 1]$ is a hyperparameter controlling the trade-off between prioritizing low-consensus samples (hallucination correction) and representative samples (cluster centrality), which we have further discussions in Section.5.2. The sample with the highest score in each cluster are selected.

4 Experiments and Results

4.1 Setup

We evaluate NEUFS against six baselines and their variants using four instruction-tuned LLMs (Llama3 3B/8B and Qwen3 4B/8B) (Grattafiori et al., 2024; Yang et al., 2025) on three reasoning and classification datasets: MMLU-Pro (Wang et al., 2024), Edu-Feedback (Wu and Schunn, 2023), and TREC (Li and Roth, 2002), stats are in Table 5. We use non-reasoning mode with 5, 10, 20, and 30 shots, averaged over three inference runs with different seeds.

Moreover, we categorize methods by their Information Type, which denotes the source of information used for selection. These categories include *Semantic* signals from external embedding models, *Entropy* from output logits, *Linguistic*[3], and our proposed neuron activation patterns. Specifically, when combining different features, we compute a unified distance for the sample selection process by summing the distances derived from each feature.

[3]We extract sparse logical linguistic feature for feature augmentation, as demonstrated in Appendix.B

4.2 Datasets

We evaluated NEUFS and baselines on three datasets from reasoning to classification tasks:

- **MMLU-Pro** (Wang et al., 2024). An advanced reasoning benchmark comprising 12,034 samples across 14 domains, which comprises ten options per question.
- **Edu-Feedback** (Wu and Schunn, 2023). A binary classification dataset for evaluating feedback quality (explanatory vs. non-explanatory) in educational systems. Collected from a real essay writing course, we split the annotated data into 1,799 training and 14,228 testing samples.
- **TREC** (Li and Roth, 2002). A 6-way question classification dataset. It consists of short open-domain questions labeled into six classes, split into 5,452 training and 500 testing samples.

4.3 Baselines

We compare NEUFS against six AFSL baselines:

- **Random.** Random selection with fixed seed.
- **Entropy.** Selects samples based on predictive uncertainty derived from output logits. We evaluate *Highest-Entropy* (ranking samples by entropy score) and *Diverse-Entropy* (stratified sampling across entropy bins).
- **TypiClust** (Hacohen et al., 2022). A semantic-only approach that encodes text via BERT and selects representative samples with K-Means.
- **Patron** (Yu et al., 2023b). Combines uncertainty and semantic. It applies graph-based uncertainty propagation to reduce entropy outliers before performing clustering selection.
- **FastVoteK** (Hongjin et al., 2022). A semantic diversity method that constructs a graph to select samples maximizing mutual distances.
- **VoteK** (Hongjin et al., 2022). Extension of FastVoteK, selects samples from diverse entropy bins to consider uncertainty.

4.4 Results

By comparing methods across various **Info Types**, as detailed below, we show that shifting from output-level signals to internal neuron dynamics consistently yields better performance.

(a) 8B Models			
Method	InfoType	Llama-3.1-8B	Qwen3-8B
Random	N/A	*0.325*$_{\pm 0.007}$	0.388$_{\pm 0.079}$
Patron	S.+E.	0.313$_{\pm 0.013}$	*0.416*$_{\pm 0.074}$
Entropy	Highest	0.317$_{\pm 0.007}$	0.394$_{\pm 0.095}$
	Diverse	0.324$_{\pm 0.003}$	0.392$_{\pm 0.066}$
TypiClust	S.	0.323$_{\pm 0.007}$	0.398$_{\pm 0.085}$
	L.	0.322$_{\pm 0.006}$	0.382$_{\pm 0.072}$
	S.+L.	0.318$_{\pm 0.006}$	0.383$_{\pm 0.087}$
FastVoteK	S.	0.316$_{\pm 0.004}$	0.379$_{\pm 0.103}$
	L.	0.323$_{\pm 0.003}$	0.373$_{\pm 0.089}$
	S.+L.	0.318$_{\pm 0.009}$	0.402$_{\pm 0.075}$
VoteK	S.+E.	0.318$_{\pm 0.004}$	0.391$_{\pm 0.068}$
	S.+E.+L.	0.309$_{\pm 0.007}$	0.402$_{\pm 0.075}$
NeuFS	Neuron	**0.327**$_{\pm 0.007}$	**0.418**$_{\pm 0.069}$

(b) 3B & 4B Models			
Method	InfoType	Llama-3.2-3B	Qwen3-4B
Random	N/A	*0.249*$_{\pm 0.005}$	0.412$_{\pm 0.015}$
Patron	S.+E.	0.244$_{\pm 0.009}$	0.391$_{\pm 0.045}$
Entropy	Highest	0.245$_{\pm 0.005}$	0.430$_{\pm 0.024}$
	Diverse	0.244$_{\pm 0.012}$	0.414$_{\pm 0.019}$
TypiClust	S.	0.242$_{\pm 0.005}$	*0.437*$_{\pm 0.016}$
	L.	0.248$_{\pm 0.003}$	0.376$_{\pm 0.026}$
	S.+L.	0.243$_{\pm 0.004}$	0.398$_{\pm 0.028}$
FastVoteK	S.	0.245$_{\pm 0.001}$	0.386$_{\pm 0.017}$
	L.	0.242$_{\pm 0.002}$	0.401$_{\pm 0.026}$
	S.+L.	0.242$_{\pm 0.003}$	0.420$_{\pm 0.014}$
VoteK	S.+E.	0.246$_{\pm 0.003}$	0.401$_{\pm 0.012}$
	S.+E.+L.	0.233$_{\pm 0.008}$	0.374$_{\pm 0.012}$
NeuFS	Neuron	**0.251**$_{\pm 0.005}$	**0.452**$_{\pm 0.010}$

Table 1: Average accuracy ($\pm$ standard deviation) on the MMLU-Pro, aggregated across 5, 10, 20, and 30-shot settings. **Bold** and *italics* indicate the best and second-best performance, respectively. InfoType denotes the source of information used for selection: Semantic (S.), Entropy (E.), Linguistic (L.), and Neuron activations.

Results on Reasoning Task. Table 1 highlights the limitations of traditional information types in complex reasoning scenarios, i.e MMLU-Pro. While methods relying on Semantic signals like TypiClust improve over random selection, they are consistently outperformed by NEUFS. By utilizing the Neuron Info, NEUFS achieves the highest accuracy of 0.452 on Qwen3-4B and 0.418 on Qwen3-8B. It is worth noting that NEUFS also surpasses Patron, a method combining both semantic and entropy signals. This result suggests that internal neuron consensus provides a more reliable signal for demonstration selection than combining external semantic density with predictive uncertainty.

Results on Classification Task. The advantage of the neuron-aware selection strategy consistency brings performance rises to classification tasks as shown in Table 2 and Table 3.

For 8B models shown in Table 2, NEUFS consistently outperforms baselines that rely on entropy information. On the Edu-Feedback dataset, the proposed NEUFS outperforms all other baselines in terms of accuracy with both Llama3 and Qwen3 models, with competitive Macro-F1 values. Similarly, on the TREC dataset, the proposed NeuFS demonstrated state-of-the-art performances in both F1 values and accuracies with Qwen3-8B.

For 4B-level LLMs, this trend persists as presented in Table 3. NEUFS demonstrates substantial gains in specialized domains. For instance, on the Edu-Feedback task with Qwen3-4B, it achieves a F1 of 0.692, significantly outperforming TypiClust and Highest-Entropy-based methods. While some baselines like Fast-VoteK (S.+L.) appear competitive on datasets like TREC, these methods often depend on the participation of external knowledge. NEUFS's ability to achieve superior results using only internal neuron dynamics proves its efficacy as a more principled, model-aware selection strategy.

Rather than relying on surface-level cues such as semantic similarity or output probabilities, NEUFS directly leverages the model's internal neuron activations to select informative examples for learning. It promotes diversity by identifying distinct activation patterns that capture complementary knowledge, and employs a neuron-consensus score to pinpoint instances where the model is most prone to errors or hallucinations. By explicitly targeting internal knowledge gaps, NEUFS improves sample efficiency and often outperforms prior selection strategies, particularly for domain-specific tasks.

5 Ablation Study

5.1 Representation Variants

To validate the effectiveness of using sparse neuron activations as sample representations, we compare NEUFS against various dense vector representations. We compare with both *Encoder-based* and *Decoder-based* models. For Encoder-based representations, we utilize SimCSE (Gao et al., 2021), a sentence embedding model based on BERT. For Decoder-based representations, we utilizes the Qwen-Embedding-0.6B, which is specifically designed to generate high-quality text embeddings aligned with the Qwen series LLMs.

Model		Llama-3.1-8B				Qwen3-8B			
Method	InfoType	Edu-Feedback		TREC		Edu-Feedback		TREC	
		Macro-F1	Acc	Macro-F1	Acc	Macro-F1	Acc	Macro-F1	Acc
Random	N/A	$0.645_{\pm 0.053}$	$0.662_{\pm 0.065}$	$0.777_{\pm 0.052}$	$0.764_{\pm 0.070}$	$0.612_{\pm 0.084}$	$0.625_{\pm 0.097}$	$0.844_{\pm 0.022}$	$0.823_{\pm 0.030}$
Patron	S.+E.	$0.643_{\pm 0.027}$	$0.690_{\pm 0.025}$	$0.807_{\pm 0.046}$	$0.809_{\pm 0.045}$	$0.659_{\pm 0.022}$	*0.709 ±0.037*	$0.825_{\pm 0.023}$	$0.824_{\pm 0.017}$
Entropy	Highest	$0.619_{\pm 0.027}$	$0.625_{\pm 0.030}$	$0.790_{\pm 0.029}$	$0.785_{\pm 0.031}$	$0.555_{\pm 0.049}$	$0.557_{\pm 0.051}$	$0.837_{\pm 0.035}$	$0.839_{\pm 0.031}$
	Diverse	**0.670 ±0.028**	*0.696 ±0.029*	$0.829_{\pm 0.030}$	**0.827 ±0.033**	$0.632_{\pm 0.035}$	$0.663_{\pm 0.070}$	$0.856_{\pm 0.012}$	$0.841_{\pm 0.017}$
TypiClust	S.	$0.642_{\pm 0.049}$	$0.683_{\pm 0.071}$	$0.798_{\pm 0.026}$	$0.791_{\pm 0.035}$	$0.605_{\pm 0.106}$	$0.629_{\pm 0.122}$	$0.831_{\pm 0.022}$	$0.828_{\pm 0.022}$
	L.	*0.664 ±0.014*	$0.695_{\pm 0.021}$	$0.806_{\pm 0.026}$	$0.802_{\pm 0.038}$	$0.626_{\pm 0.025}$	$0.637_{\pm 0.033}$	$0.835_{\pm 0.030}$	$0.826_{\pm 0.040}$
	S.+L.	$0.623_{\pm 0.055}$	$0.637_{\pm 0.066}$	$0.814_{\pm 0.030}$	$0.804_{\pm 0.039}$	$0.589_{\pm 0.091}$	$0.600_{\pm 0.101}$	$0.851_{\pm 0.008}$	$0.835_{\pm 0.005}$
FastVoteK	S.	$0.658_{\pm 0.012}$	$0.694_{\pm 0.004}$	$0.828_{\pm 0.024}$	*0.825 ±0.030*	$0.640_{\pm 0.027}$	$0.662_{\pm 0.038}$	$0.840_{\pm 0.017}$	$0.831_{\pm 0.021}$
	L.	$0.654_{\pm 0.027}$	$0.676_{\pm 0.032}$	*0.832 ±0.046*	*0.825 ±0.048*	$0.621_{\pm 0.059}$	$0.632_{\pm 0.066}$	$0.854_{\pm 0.018}$	$0.843_{\pm 0.017}$
	S.+L.	$0.657_{\pm 0.042}$	$0.688_{\pm 0.058}$	$0.809_{\pm 0.051}$	$0.813_{\pm 0.052}$	$0.614_{\pm 0.097}$	$0.631_{\pm 0.108}$	*0.861 ±0.022*	*0.854 ±0.011*
VoteK	S.+E.	$0.660_{\pm 0.028}$	$0.692_{\pm 0.027}$	*0.832 ±0.019*	$0.822_{\pm 0.020}$	**0.668 ±0.020**	$0.701_{\pm 0.021}$	$0.839_{\pm 0.006}$	$0.839_{\pm 0.010}$
	S.+E.+L.	$0.653_{\pm 0.043}$	$0.676_{\pm 0.054}$	$0.818_{\pm 0.052}$	$0.810_{\pm 0.051}$	$0.631_{\pm 0.032}$	$0.648_{\pm 0.047}$	$0.839_{\pm 0.006}$	$0.826_{\pm 0.022}$
NeuFS	Neuron	$0.660_{\pm 0.024}$	**0.698 ±0.016**	**0.834 ±0.030**	$0.823_{\pm 0.036}$	*0.663 ±0.014*	**0.711 ±0.019**	**0.862 ±0.027**	**0.858 ±0.020**

Table 2: Average performances ($\pm$ standard deviation) on the TREC and Edu-Feedback datasets with 8B models. **Bold** and *italics* indicate the best and second-best performance, respectively.

Model		Llama-3.2-3B				Qwen3-4B			
Method	InfoType	Edu-Feedback		TREC		Edu-Feedback		TREC	
		Macro-F1	Acc	Macro-F1	Acc	Macro-F1	Acc	Macro-F1	Acc
Random	N/A	$0.557_{\pm 0.029}$	$0.558_{\pm 0.030}$	$0.699_{\pm 0.041}$	$0.707_{\pm 0.049}$	$0.653_{\pm 0.080}$	$0.667_{\pm 0.094}$	$0.859_{\pm 0.037}$	$0.860_{\pm 0.037}$
Patron	S.+E.	$0.569_{\pm 0.111}$	$0.597_{\pm 0.134}$	$0.727_{\pm 0.051}$	$0.749_{\pm 0.033}$	*0.685 ±0.027*	**0.742 ±0.030**	$0.842_{\pm 0.023}$	$0.853_{\pm 0.024}$
Entropy	Highest	$0.501_{\pm 0.080}$	$0.506_{\pm 0.074}$	$0.663_{\pm 0.022}$	$0.638_{\pm 0.030}$	$0.555_{\pm 0.065}$	$0.557_{\pm 0.064}$	$0.855_{\pm 0.012}$	$0.857_{\pm 0.014}$
	Diverse	**0.657 ±0.034**	**0.671 ±0.042**	$0.736_{\pm 0.048}$	$0.759_{\pm 0.020}$	$0.671_{\pm 0.056}$	$0.684_{\pm 0.066}$	$0.862_{\pm 0.019}$	$0.867_{\pm 0.013}$
TypiClust	S.	$0.545_{\pm 0.107}$	$0.557_{\pm 0.116}$	$0.741_{\pm 0.049}$	$0.744_{\pm 0.039}$	$0.626_{\pm 0.095}$	$0.640_{\pm 0.111}$	$0.853_{\pm 0.014}$	$0.866_{\pm 0.003}$
	L.	$0.606_{\pm 0.096}$	$0.624_{\pm 0.116}$	$0.712_{\pm 0.030}$	$0.740_{\pm 0.069}$	$0.636_{\pm 0.015}$	$0.642_{\pm 0.017}$	$0.862_{\pm 0.008}$	$0.863_{\pm 0.008}$
	S.+L.	$0.537_{\pm 0.033}$	$0.538_{\pm 0.033}$	$0.753_{\pm 0.042}$	$0.750_{\pm 0.049}$	$0.613_{\pm 0.086}$	$0.623_{\pm 0.096}$	$0.855_{\pm 0.020}$	$0.858_{\pm 0.013}$
FastVoteK	S.	$0.507_{\pm 0.046}$	$0.509_{\pm 0.044}$	**0.760 ±0.026**	$0.761_{\pm 0.030}$	$0.673_{\pm 0.029}$	$0.707_{\pm 0.047}$	**0.873 ±0.010**	*0.871 ±0.008*
	L.	$0.548_{\pm 0.104}$	$0.555_{\pm 0.101}$	$0.718_{\pm 0.044}$	$0.739_{\pm 0.042}$	$0.662_{\pm 0.046}$	$0.673_{\pm 0.096}$	$0.861_{\pm 0.027}$	$0.867_{\pm 0.017}$
	S.+L.	$0.541_{\pm 0.059}$	$0.543_{\pm 0.061}$	$0.726_{\pm 0.034}$	*0.775 ±0.017*	$0.655_{\pm 0.083}$	$0.679_{\pm 0.054}$	$0.847_{\pm 0.026}$	$0.857_{\pm 0.025}$
VoteK	S.+E.	$0.526_{\pm 0.027}$	$0.528_{\pm 0.029}$	$0.755_{\pm 0.035}$	$0.771_{\pm 0.023}$	$0.664_{\pm 0.044}$	$0.681_{\pm 0.056}$	$0.853_{\pm 0.007}$	$0.850_{\pm 0.012}$
	S.+E.+L.	$0.572_{\pm 0.065}$	$0.577_{\pm 0.076}$	*0.757 ±0.025*	**0.776 ±0.024**	$0.681_{\pm 0.055}$	$0.702_{\pm 0.067}$	$0.854_{\pm 0.037}$	$0.846_{\pm 0.023}$
NeuFS	Neuron	*0.624 ±0.007*	*0.636 ±0.008*	$0.754_{\pm 0.032}$	$0.761_{\pm 0.044}$	**0.692 ±0.021**	*0.725 ±0.038*	*0.865 ±0.019*	**0.878 ±0.015**

Table 3: Average performances ($\pm$ standard deviation) on the TREC and Edu-Feedback datasets with 3B and 4B models. **Bold** and *italics* indicate the best and second-best performance, respectively.

#Shot	NeuFS w/ Qwen-Embed[4]	NeuFS w/ simcse	NeuFS
MMLU-Pro			
5	$0.2851_{\pm 0.0211}$	**0.3598 ±0.0158**	$0.3341_{\pm 0.0232}$
10	$0.3823_{\pm 0.0113}$	$0.3667_{\pm 0.0129}$	**0.3911 ±0.0117**
20	$0.4517_{\pm 0.0040}$	**0.4622 ±0.0073**	$0.4593_{\pm 0.0054}$
30	$0.4863_{\pm 0.0039}$	$0.4638_{\pm 0.0052}$	**0.4866 ±0.0036**
Avg.	$0.4013_{\pm 0.0887}$	$0.4131_{\pm 0.0577}$	**0.4178 ±0.0687**
Edu-Feedback			
5	$0.6362_{\pm 0.0018}$	$0.6308_{\pm 0.0009}$	**0.7088 ±0.0009**
10	$0.6492_{\pm 0.0018}$	$0.6827_{\pm 0.0013}$	**0.6928 ±0.0014**
20	$0.5990_{\pm 0.0020}$	**0.7219 ±0.0002**	$0.7033_{\pm 0.0012}$
30	$0.7162_{\pm 0.0005}$	$0.7118_{\pm 0.0016}$	**0.7378 ±0.0004**
Avg.	$0.6502_{\pm 0.0489}$	$0.6868_{\pm 0.0409}$	**0.7107 ±0.0193**
TREC			
5	**0.8620 ±0.0000**	$0.8433_{\pm 0.0031}$	$0.8287_{\pm 0.0031}$
10	$0.8533_{\pm 0.0050}$	$0.7847_{\pm 0.0012}$	**0.8727 ±0.0012**
20	$0.8027_{\pm 0.0023}$	$0.7667_{\pm 0.0031}$	**0.8600 ±0.0020**
30	$0.8447_{\pm 0.0031}$	$0.7847_{\pm 0.0031}$	**0.8687 ±0.0023**
Avg.	$0.8407_{\pm 0.0263}$	$0.7948_{\pm 0.0334}$	**0.8575 ±0.0199**

Table 4: Representation model variants.

As presented in Table 4, results demonstrate that NEUFS consistently outperforms both dense representation variants. While the Decoder-based Qwen generally surpasses the Encoder-based baseline SimCSE, it still underperforms compared to our neuron-aware method. This confirms that the specific information provided by neuron activations, which directly links to knowledge circuits, is more effective for few-shot selection than the coarse-grained semantic proximity offered by dense vectors on reasoning and classification tasks.

5.2 Impact of Neuron Sparsity k

The parameter k determines the sparsity of the neuron representation $\mathcal{N}_{act}$. We vary k from 2,000 to 10,000 to analyze how the granularity of the internal signal affects selection quality.

As illustrated in Figure 3, the overall performance fluctuation is relatively mild, suggesting that NEUFS is generally robust to the specific activation threshold. However, we observe a distinct difference in sensitivity between model sizes: the smaller Qwen3-4B model exhibits more noticeable performance variance compared to the Qwen3-8B, which remains highly stable across the spectrum. This indicates that while larger models may possess redundant knowledge circuits that buffer against selection noise, smaller models are more sensitive

to noises and the selection of k.

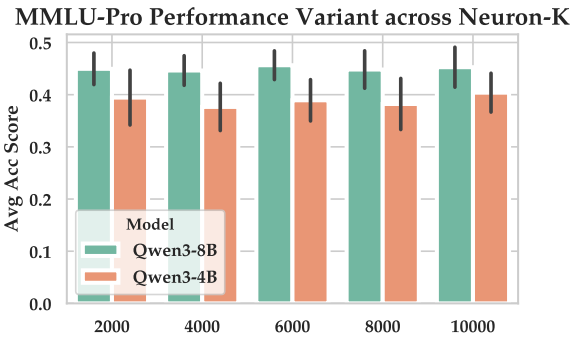

Figure 3: Ablation study on the k which used to define the activation threshold. The bar plot shows average performance across 5,10,20,30 shots on Qwen3 series.

5.3 Impact of Sample Scoring Weight τ

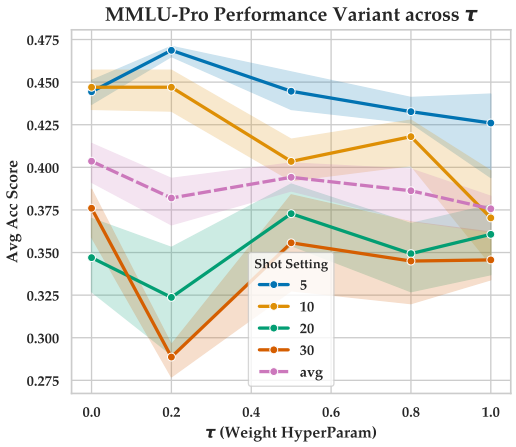

(a) Performance on Qwen3 4B

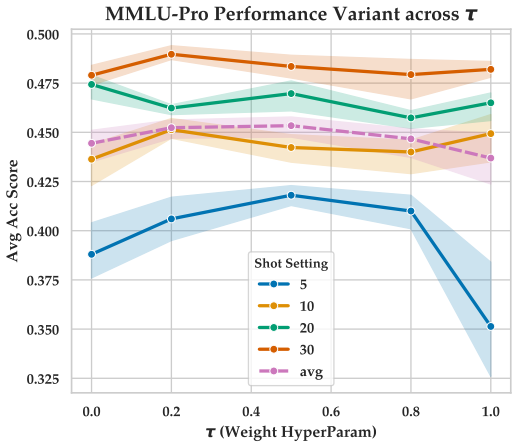

(b) Performance on Qwen3 8B

Figure 4: Ablation study on the weight hyper-parameter τ across different model sizes. The shaded regions represent the standard deviation across three runs.

The hyperparameter τ governs the trade-off between maximizing representativeness via cluster centric distance, which becomes dominant when τ approaches zero, and minimizing hallucination risk through Neuron Consensus, which prevails when τ approaches one. We analyze the impact of τ on model performance separately for different model sizes, as illustrated in Figure 4.

For 4B-level models. As shown in Figure 4(a), the smaller model exhibits significant volatility across different weight settings. Crucially, though NEUFS achieved satisfying performance when τ is set to 0.5, the average performance represented by the dashed purple line achieves its maximum value when τ is set to 0, indicating that the 4B model could benefits most from pure sample diversification. As τ increases, performance fluctuates and generally declines. This suggests that neuron consensus signals could be noisier in smaller models. Less capacity leads to higher uncertainty across most candidates, reducing signal reliability and distinguishability. As a result, diversity and representativeness derived from neuron features become the dominant factors in AFSL.

For 8B-level models. In contrast, the larger model in Figure 4(b) displays a much smoother trend. The average performance clearly benefits from the integration of internal signals, peaking when τ is 0.5. This indicates that for 8B models, which likely possess more stable and meaningful internal representations, the neuron consensus metric effectively complements diversity. However, similar to the 4B model, pushing τ to 1 causes a sharp drop, confirming that while consensus is valuable, it cannot entirely replace diversity coverage.

6 Conclusion

In this work, we introduced NEUFS, an AFSL framework that shifts the selection paradigm from output-level signals to internal neuron dynamics. By leveraging activation patterns, we proposed a dual-criteria scoring method that combines *Neuron-Aware Sample Diversification* for coverage with *Neuron Consensus* for hallucination mitigation. Experiments on reasoning and classification tasks confirm NEUFS's superiority over baselines, validating internal signals offer greater robustness than traditional similarity and output-level uncertainty metrics. Beyond performance gains, this work highlights the critical role of model internal dynamics in data selection, encouraging future research to leverage internal model states for designing more robust and theoretically grounded strategies.

Limitations

Despite the effectiveness of NEUFS, we acknowledge several limitations. The proposed framework relies on accessing internal FFN activations and unembedding matrices, limiting its applicability to open-weights models rather than black-box APIs. Also, while we employ two-stage filtering for efficiency, analyzing neuron patterns across large unlabeled pools incurs higher computational overhead compared to retrieving static pre-computed embeddings.

A Experiments

A.1 Experiment Settings.

We experimented with 5, 10, 20, and 30 examples in few-shot setting and report the average performance. All experiments are done with the VLLM (Kwon et al., 2023) framework on four A100s, with a fixed temperature of 0.6. All reported results are averaged cross three runs, each with a different random seed.

A.2 Baseline Algorithms

To perform comparison on various CSAL algorithms, we selected six baseline methods, as follows.

- **Random.** We apply the random package in Python with a fix seed of 42 to perform 5, 10, 20, and 30 shot demonstration selection.
- **Entropy.** For entropy, we apply both highest-entropy and diverse-entropy selection strategies. We begin by extracting LLMs' entropies using a few-shot prompting approach with 5 randomly sampled shots. The entropies are then computed from the output logits. For highest-entropy selection, following prior work (Schröder et al., 2021), we rank all samples by their entropy values and select the top 5, 10, 20, and 30 samples. For diverse-entropy selection, we partition the samples into multiple bins according to the number of shots, and then randomly select one sample from each bin to construct the final dataset.
- **TypiClust** (Hacohen et al., 2022). The method that purely considers the semantic information. Typiclust firstly encodes all textual samples with text representation models such as BERT, then performs unsupervised clustering with the classic KMeans algorithm, with the cluster number being set to the same as number of shots. Finally it selects sample from each cluster.
- **Fast-Votek** (Hongjin et al., 2022). This method is purely semantic-based, which performs a graph construction with semantic distances and the K nearest neighbour algorithm, then selects samples that could maximize the distances between all samples in the selected set.
- **Patron** (Yu et al., 2023b), which simultaneously considers both entropy information and semantic information. It constructed a graph based on semantic distances, then performed uncertainty propagation on the graph, which mitigates entropy outliers. Finally, it performs unsupervised clustering, selecting a sample from each cluster.
- **Votek** (Hongjin et al., 2022), in addition to fast-votek, this algorithm incrementally considers the entropy information, selecting samples across different levels of entropy bins.

A.3 Datasets

We used three datasets in our work, all data are anonymized.

Edu-Feedback. Explanatory peer-feedback classification is a binary text classification dataset, which distinguishes comments with explicit rationales from non-explanatory ones, serving as a key measure of review quality. It is a crucial task in building educational AI systems.

We collected and annotated more than 14,000 review samples from a real essay writing course. For experiments, we take 1799 samples as the training set, and the rest 14,228 samples as the testing set.

TREC. We use the TREC question classification dataset, coarse-grained, 6-way. It contains 5,452 training and 500 testing questions, each labeled with one of six categories: *ABBR*, *DESC*, *ENTY*, *HUM*, *LOC*, and *NUM*. Each instance is a short, open-domain question.

MMLU-Pro. MMLU-Pro is an enhanced version of the Massive Multitask Language Understanding (MMLU) benchmark. It increases the difficulty by expanding the candidate options from 4 to 10 and focusing on more complex, reasoning-intensive questions across 14 diverse domains. This dataset

provides a more robust evaluation of a model's advanced knowledge and analytical capabilities compared to the original benchmark. For experiments, we randomly selected 2000 samples as the candidate pool and the rest samples as the testing set.

Dataset	Source Domain	#Class	#Candidate	#Test
MMLU-Pro	Multi-disciplinary	10	2000	10032
Edu-Feedback	Peer-feedback	2	1799	14228
TREC	Question	6	5452	500

Table 5: Data Statistics.

A.4 Hyper-parameter Settings

Here we provide the hyper-parameter setting for the hyperparameter K, which defines the threshold for activation neuron identification in Equation.3, and the hyperparameter τ, which defines the weighting parameter in Equation.6.

Model	K	τ
MMLU-Pro		
Llama-3.1-8B	6000	0.8
Llama-3.2-3B	6000	1
Qwen3-8B	8000	0.5
Qwen3-4B-Instruct-2507	8000	0.5
Edu-Feedback		
Llama-3.1-8B	500	0.2
Llama-3.2-3B	1000	1
Qwen3-8B	1000	0.5
Qwen3-4B-Instruct-2507	4000	0.5
TREC		
Llama-3.1-8B	3000	0.25
Llama-3.2-3B	4000	0.5
Qwen3-8B	5000	1
Qwen3-4B-Instruct-2507	5000	1

Table 6: Hyper-parameter Setting

A.5 Results

We demonstrated the complete experimental results from Table.7 to Table.12.

B Linguistic Features.

To incorporate additional linguistic information, we extract sparse linguistic features and integrate them into the selection process. We collect three types of linguistic features: count-based, Rhetorical Structure Theory (RST) (Mann and Thompson, 1988) features and topical features. For count-based features, we count number of indicator features such as causal markers, rhetorical terms, relative clauses, critique and praise expressions, and action verbs.[5] For RST-based feature, we employed Qwen3-Next-80B (Yang et al., 2025) to get the RST tree labels, then representing the results with a count-based vector. For RST Analysis, conversational example is demonstrated in Figure.5.

Prompt

```
You are a Rhetorical Structure Theory discourse parser for English text.
Follow these steps internally, but output only valid JSON.

### Task
1. Split the input text into **Elementary Discourse Units (EDUs)** — minimal
discourse segments (clauses or short sentences).
2. Identify **Rhetorical Relations** between EDUs. Allowed relation types are
strictly limited to:
  - Causal / Logical Relations
    - Cause–Effect: One span presents a cause, the other its effect.
    - Condition: One span sets a condition under which the other holds.
    - Concession: One span acknowledges a contrary point, while the other still
holds.
  - Elaborative / Explanatory Relations
    - Elaboration: One span adds detail to another (examples, restatements,
specifics).
    - Evidence: One span supports the truth or plausibility of another.
    - Justify: Provides reasons for the writer's intention to assert something.
  - Contrastive Relations
    - Contrast: Two spans highlight differences or opposites.
    - Antithesis: One span is strengthened by contrasting it with an opposite idea.
  - Temporal / Sequential Relations
    - Sequence: Events or actions follow each other in order.
    - Circumstance: One span sets the background situation for another.
  - Additive / Associative Relations
    - List: Multiple spans presented as coordinate items.
    - Joint: Spans contribute equally to the discourse, without hierarchy.
  - Preparatory / Framing Relations
    - Background: Provides context needed to understand another span.
    - Preparation: Introduces or primes the reader for what comes next.

3. For each relation:
  - **Asymmetric relations** (Cause, Elaboration, Condition, Purpose, Background,
Other):
    use `"nucleus"` and `"satellite"` to indicate main vs. supporting unit.
  - **Symmetric relations** (Contrast, Sequence):
    use `"span1"` and `"span2"` to indicate the two nucleus spans.
4. Output must be a single valid **JSON object** containing:
  - `"EDUs"`: list of EDU strings (in original order).
  - `"Relations"`: list of relation objects following the above format.
5. Do not include explanations, comments, or text outside the JSON.
```

User

"I didn't bring an umbrella because the forecast said it would be sunny."

Assistant

```
{
  "EDUs": [
    "I didn't bring an umbrella",
    "because the forecast said it would be sunny"
  ],
  "Relations": [
    {"type": "Cause", "nucleus": "I didn't bring an umbrella", "satellite": "because the
forecast said it would be sunny"}
  ]
}
```

Figure 5: Example for RST Analysis.

For topical analysis, we segmented long text into short sentences, clustered them with K-Means, and finally vectorized each sample using counts to obtain sparse features.

References

Saeed Ahmadnia, Arash Yousefi Jordehi, Mahsa Hosseini Khasheh Heyran, Seyed Abolghasem Mirroshandel, Owen Rambow, and Cornelia Caragea. 2025. Active few-shot learning for text classification. *arXiv preprint arXiv:2502.18782*.

[5] NLTK (https://www.nltk.org) is employed for data processing, keyword dictionaries are manually defined.

Method	#Shot	5		10		20		30		Avg.	
	InfoType	Macro-F1	Acc	Macro-F1	Acc	Macro-F1	Acc	Macro-F1	Acc	Macro-F1	Acc
Llama-3.1-8B-Instruct											
Random	N/A	0.3401±0.0142	0.3292±0.0193	0.3428±0.0179	0.3318±0.0231	0.3309±0.0277	0.3208±0.0347	0.3270±0.0235	0.3165±0.0291	0.3352±0.0075	0.3246±0.0072
Patron	S.+E.	0.3418±0.0117	0.3305±0.0177	0.3275±0.0213	0.3157±0.0276	0.3135±0.0317	0.3020±0.0362	0.3135±0.0336	0.3055±0.0392	0.3241±0.0135	0.3134±0.0128
Entropy	Highest	0.3358±0.0088	0.3236±0.0139	0.3297±0.0280	0.3205±0.0325	0.3242±0.0317	0.3163±0.0366	0.3147±0.0322	0.3066±0.0354	0.3261±0.0090	0.3167±0.0074
	Diverse	0.3379±0.0183	0.3266±0.0252	0.3302±0.0269	0.3194±0.0334	0.3355±0.0261	0.3248±0.0334	0.3354±0.0190	0.3243±0.0252	0.3348±0.0033	0.3237±0.0031
TypiClust	S.	0.3411±0.0199	0.3321±0.0258	0.3371±0.0196	0.3262±0.0252	0.3281±0.0255	0.3174±0.0311	0.3282±0.0226	0.3172±0.0302	0.3336±0.0065	0.3232±0.0073
	L.	0.3387±0.0201	0.3293±0.0258	0.3344±0.0248	0.3247±0.0292	0.3291±0.0290	0.3188±0.0338	0.3273±0.0265	0.3165±0.0335	0.3324±0.0052	0.3223±0.0058
	S.+L.	0.3350±0.0183	0.3260±0.0243	0.3250±0.0259	0.3145±0.0307	0.3249±0.0296	0.3150±0.0332	0.3248±0.0285	0.3145±0.0347	0.3274±0.0050	0.3175±0.0057
fast-votek	S.	0.3307±0.0201	0.3211±0.0246	0.3234±0.0306	0.3137±0.0336	0.3247±0.0280	0.3160±0.0337	0.3222±0.0280	0.3134±0.0329	0.3252±0.0038	0.3160±0.0035
	L.	0.3349±0.0226	0.3268±0.0280	0.3318±0.0287	0.3216±0.0338	0.3305±0.0244	0.3209±0.0292	0.3331±0.0238	0.3238±0.0294	0.3326±0.0019	0.3233±0.0026
	S.+L.	0.3367±0.0229	0.3281±0.0277	0.3332±0.0260	0.3235±0.0295	0.3209±0.0361	0.3123±0.0384	0.3190±0.0301	0.3086±0.0339	0.3275±0.0088	0.3181±0.0092
votek	S.+E.	0.3308±0.0223	0.3210±0.0266	0.3261±0.0265	0.3161±0.0304	0.3312±0.0278	0.3212±0.0322	0.3229±0.0302	0.3128±0.0359	0.3277±0.0040	0.3178±0.0041
	S.+E.+L.	0.3232±0.0272	0.3142±0.0289	0.3258±0.0263	0.3145±0.0301	0.3139±0.0294	0.3021±0.0331	0.3137±0.0333	0.3039±0.0387	0.3191±0.0063	0.3087±0.0066
NeuronPattern	Neuron	0.3463±0.0124	0.3371±0.0174	0.3374±0.0144	0.3263±0.0182	0.3321±0.0227	0.3224±0.0292	0.3320±0.0232	0.3229±0.0288	0.3369±0.0067	0.3272±0.0068
Llama-3.2-3B-Instruct											
Method	#Shot	5		10		20		30		Avg.	
	InfoType	Macro-F1	Acc	Macro-F1	Acc	Macro-F1	Acc	Macro-F1	Acc	Macro-F1	Acc
Random	N/A	0.2349±0.0579	0.2481±0.0470	0.2401±0.0612	0.2532±0.0499	0.2267±0.0728	0.2422±0.0566	0.2433±0.0588	0.2521±0.0479	0.2362±0.0072	0.2489±0.0050
Patron	S.+E.	0.2374±0.0601	0.2516±0.0485	0.2339±0.0553	0.2429±0.0411	0.2188±0.0725	0.2321±0.0564	0.2367±0.0702	0.2494±0.0549	0.2317±0.0087	0.2440±0.0087
Entropy	Highest	0.2343±0.0544	0.2484±0.0444	0.2361±0.0634	0.2501±0.0507	0.2239±0.0673	0.2388±0.0517	0.2276±0.0661	0.2417±0.0525	0.2305±0.0057	0.2447±0.0054
	Diverse	0.2003±0.0796	0.2261±0.0570	0.2285±0.0716	0.2469±0.0568	0.2364±0.0667	0.2507±0.0539	0.2392±0.0621	0.2501±0.0496	0.2261±0.0178	0.2435±0.0117
TypiClust	S.	0.2420±0.0520	0.2492±0.0405	0.2313±0.0649	0.2429±0.0495	0.2260±0.0596	0.2371±0.0465	0.2307±0.0557	0.2396±0.0445	0.2325±0.0068	0.2422±0.0052
	L.	0.2389±0.0509	0.2477±0.0420	0.2411±0.0543	0.2517±0.0445	0.2299±0.0698	0.2434±0.0537	0.2377±0.0632	0.2474±0.0514	0.2369±0.0049	0.2475±0.0034
	S.+L.	0.2409±0.0539	0.2483±0.0422	0.2276±0.0624	0.2379±0.0458	0.2294±0.0731	0.2427±0.0562	0.2328±0.0613	0.2421±0.0476	0.2327±0.0059	0.2428±0.0043
fast-votek	S.	0.2342±0.0552	0.2457±0.0440	0.2333±0.0578	0.2432±0.0454	0.2331±0.0610	0.2447±0.0488	0.2348±0.0578	0.2452±0.0468	0.2338±0.0008	0.2447±0.0011
	L.	0.2215±0.0806	0.2394±0.0592	0.2257±0.0792	0.2429±0.0600	0.2298±0.0720	0.2431±0.0565	0.2322±0.0675	0.2440±0.0531	0.2273±0.0047	0.2423±0.0020
	S.+L.	0.2237±0.0716	0.2379±0.0519	0.2313±0.0711	0.2458±0.0553	0.2249±0.0755	0.2408±0.0559	0.2344±0.0620	0.2431±0.0497	0.2286±0.0051	0.2419±0.0033
votek	S.+E.	0.2321±0.0503	0.2411±0.0391	0.2342±0.0609	0.2465±0.0486	0.2326±0.0714	0.2458±0.0562	0.2386±0.0616	0.2492±0.0504	0.2344±0.0029	0.2456±0.0034
	S.+E.+L.	0.2081±0.0646	0.2227±0.0482	0.2140±0.0771	0.2314±0.0568	0.2246±0.0731	0.2380±0.0558	0.2250±0.0721	0.2398±0.0559	0.2179±0.0083	0.2330±0.0078
NeuronPattern	Neuron	0.2435±0.0512	0.2561±0.0439	0.2434±0.0534	0.2534±0.0445	0.2393±0.0571	0.2499±0.0466	0.2333±0.0589	0.2447±0.0478	0.2399±0.0048	0.2510±0.0049

Table 7: Experimental results with Llama series on MMLU-Pro.

Method	#Shot	5		10		20		30		Avg.	
	InfoType	Macro-F1	Acc	Macro-F1	Acc	Macro-F1	Acc	Macro-F1	Acc	Macro-F1	Acc
Llama-3.1-8B-Instruct											
Random	N/A	0.6424±0.0048	0.6581±0.0074	0.5728±0.0101	0.5739±0.0108	0.6691±0.0042	0.6899±0.0072	0.6974±0.0037	0.7273±0.0066	0.6454±0.0534	0.6623±0.0654
Patron	S.+E.	0.6636±0.0010	0.7263±0.0041	0.6046±0.0036	0.6862±0.0032	0.6565±0.0048	0.6751±0.0078	0.6488±0.0047	0.6703±0.0080	0.6434±0.0266	0.6895±0.0254
Entropy	Highest	0.6066±0.0076	0.6128±0.0091	0.5878±0.0104	0.5897±0.0114	0.6314±0.0080	0.6384±0.0096	0.6497±0.0094	0.6571±0.0111	0.6189±0.0272	0.6245±0.0295
	Diverse	0.6447±0.0055	0.6643±0.0084	0.6468±0.0020	0.6775±0.0055	0.6907±0.0052	0.7183±0.0107	0.6967±0.0065	0.7223±0.0102	0.6697±0.0278	0.6956±0.0291
TypiClust	S.	0.5720±0.0098	0.5770±0.0117	0.6462±0.0036	0.7066±0.0043	0.6649±0.0047	0.7265±0.0021	0.6828±0.0006	0.7202±0.0065	0.6415±0.0487	0.6826±0.0709
	L.	0.6608±0.0025	0.7153±0.0040	0.6575±0.0012	0.6987±0.0045	0.6527±0.0101	0.6649±0.0127	0.6836±0.0061	0.6991±0.0081	0.6636±0.0137	0.6945±0.0212
	S.+L.	0.5600±0.0063	0.5618±0.0072	0.6000±0.0104	0.6052±0.0123	0.6466±0.0036	0.6740±0.0073	0.6857±0.0034	0.7082±0.0065	0.6231±0.0547	0.6373±0.0661
fast-votek	S.	0.6463±0.0002	0.6965±0.0061	0.6551±0.0014	0.6889±0.0052	0.6568±0.0020	0.6956±0.0070	0.6749±0.0039	0.6951±0.0066	0.6583±0.0120	0.6940±0.0035
	L.	0.6179±0.0030	0.6435±0.0069	0.6722±0.0005	0.7124±0.0044	0.6751±0.0064	0.6922±0.0088	0.6489±0.0077	0.6559±0.0089	0.6535±0.0265	0.6760±0.0319
	S.+L.	0.5953±0.0068	0.6048±0.0089	0.6775±0.0008	0.7333±0.0044	0.6646±0.0041	0.6911±0.0074	0.6900±0.0012	0.7232±0.0043	0.6568±0.0423	0.6881±0.0584
votek	S.+E.	0.6480±0.0019	0.7030±0.0036	0.6402±0.0038	0.6710±0.0075	0.6481±0.0047	0.6673±0.0074	0.7017±0.0036	0.7248±0.0064	0.6595±0.0284	0.6915±0.0274
	S.+E.+L.	0.5912±0.0089	0.5959±0.0103	0.6612±0.0026	0.7162±0.0029	0.6732±0.0059	0.6888±0.0083	0.6865±0.0055	0.7010±0.0073	0.6530±0.0425	0.6755±0.0542
NeuronPattern	Neuron	0.6303±0.0017	0.6856±0.0038	0.6531±0.0009	0.6873±0.0049	0.6710±0.0030	0.6998±0.0070	0.6865±0.0014	0.7204±0.0060	0.6602±0.0242	0.6983±0.0160
Llama-3.2-3B-Instruct											
Method	#Shot	5		10		20		30		Avg.	
	InfoType	Macro-F1	Acc	Macro-F1	Acc	Macro-F1	Acc	Macro-F1	Acc	Macro-F1	Acc
Random	N/A	0.5640±0.0094	0.5646±0.0100	0.5149±0.0093	0.5156±0.0089	0.5647±0.0130	0.5663±0.0142	0.5826±0.0166	0.5847±0.0181	0.5566±0.0291	0.5578±0.0296
Patron	S.+E.	0.6863±0.0024	0.7467±0.0023	0.6128±0.0042	0.6483±0.0084	0.4230±0.0133	0.4322±0.0112	0.5549±0.0141	0.5616±0.0173	0.5693±0.1113	0.5972±0.1335
Entropy	Highest	0.5271±0.0079	0.5272±0.0079	0.5766±0.0084	0.5795±0.0097	0.3883±0.0136	0.4039±0.0109	0.5132±0.0205	0.5139±0.0199	0.5013±0.0801	0.5061±0.0738
	Diverse	0.6363±0.0086	0.6445±0.0105	0.6607±0.0083	0.6729±0.0105	0.7040±0.0123	0.7288±0.0176	0.6277±0.0088	0.6376±0.0109	0.6572±0.0342	0.6709±0.0415
TypiClust	S.	0.4187±0.0106	0.4291±0.0087	0.6040±0.0092	0.6109±0.0112	0.6578±0.0049	0.6891±0.0108	0.4977±0.0171	0.4980±0.0174	0.5445±0.1070	0.5568±0.1158
	L.	0.7060±0.0004	0.7506±0.0036	0.6657±0.0038	0.6904±0.0071	0.5039±0.0150	0.5046±0.0145	0.5478±0.0117	0.5497±0.0132	0.6059±0.0955	0.6238±0.1158
	S.+L.	0.4947±0.0114	0.4965±0.0106	0.5653±0.0128	0.5663±0.0136	0.5255±0.0103	0.5256±0.0104	0.5616±0.0151	0.5620±0.0156	0.5368±0.0333	0.5376±0.0329
fast-votek	S.	0.5152±0.0100	0.5153±0.0100	0.5318±0.0083	0.5329±0.0090	0.5418±0.0187	0.5435±0.0205	0.4396±0.0199	0.4455±0.0173	0.5071±0.0463	0.5093±0.0441
	L.	0.5964±0.0060	0.6028±0.0077	0.6391±0.0069	0.6488±0.0087	0.5550±0.0133	0.5551±0.0137	0.4009±0.0163	0.4147±0.0133	0.5479±0.1038	0.5554±0.1013
	S.+L.	0.5348±0.0078	0.5350±0.0081	0.6116±0.0128	0.6177±0.0150	0.4673±0.0151	0.4696±0.0139	0.5495±0.0146	0.5501±0.0152	0.5408±0.0592	0.5431±0.0608
votek	S.+E.	0.5231±0.0102	0.5233±0.0105	0.4890±0.0091	0.4903±0.0085	0.5407±0.0133	0.5436±0.0155	0.5509±0.0095	0.5552±0.0113	0.5259±0.0271	0.5281±0.0285
	S.+E.+L.	0.5393±0.0097	0.5394±0.0097	0.6698±0.0044	0.6908±0.0072	0.5423±0.0124	0.5425±0.0125	0.5368±0.0145	0.5370±0.0147	0.5721±0.0652	0.5774±0.0756
NeuronPattern	Neuron	0.6340±0.0042	0.6470±0.0062	0.6197±0.0087	0.6305±0.0113	0.6203±0.0054	0.6340±0.0084	0.6218±0.0080	0.6304±0.0100	0.6240±0.0068	0.6355±0.0079

Table 8: Experimental results with Llama series on Edu-Feedback.

Method	#Shot	5		10		20		30		Avg.	
	InfoType	Macro-F1	Acc	Macro-F1	Acc	Macro-F1	Acc	Macro-F1	Acc	Macro-F1	Acc
Llama-3.1-8B-Instruct											
Random	N/A	0.7084±0.0195	0.7020±0.0072	0.7998±0.0155	0.7827±0.0170	0.7698±0.0115	0.7160±0.0151	0.8311±0.0112	0.8553±0.0129	0.7773±0.0523	0.7640±0.0703
Patron	S.+E.	0.7563±0.0237	0.7480±0.0151	0.7817±0.0063	0.8020±0.0035	0.8550±0.0153	0.8440±0.0120	0.8343±0.0067	0.8420±0.0020	0.8068±0.0457	0.8090±0.0450
Entropy	Highest	0.8000±0.0120	0.7793±0.0162	0.8231±0.0098	0.8287±0.0081	0.7798±0.0152	0.7733±0.0170	0.7554±0.0173	0.7567±0.0081	0.7896±0.0288	0.7845±0.0310
	Diverse	0.7936±0.0150	0.7807±0.0189	0.8535±0.0098	0.8413±0.0081	0.8532±0.0079	0.8560±0.0080	0.8150±0.0088	0.8300±0.0231	0.8288±0.0296	0.8270±0.0327
TypiClust	S.	0.7759±0.0105	0.7440±0.0087	0.8031±0.0124	0.8067±0.0070	0.7810±0.0098	0.7867±0.0046	0.8320±0.0100	0.8247±0.0115	0.7980±0.0255	0.7905±0.0347
	L.	0.8035±0.0119	0.7927±0.0110	0.7733±0.0076	0.7533±0.0160	0.8362±0.0037	0.8360±0.0053	0.8121±0.0021	0.8267±0.0050	0.8063±0.0260	0.8022±0.0375
	S.+L.	0.7916±0.0053	0.7787±0.0070	0.8131±0.0024	0.8180±0.0035	0.7931±0.0144	0.7660±0.0156	0.8569±0.0034	0.8527±0.0058	0.8137±0.0304	0.8038±0.0394
fast-votek	S.	0.7945±0.0075	0.7867±0.0095	0.8425±0.0012	0.8400±0.0020	0.8243±0.0161	0.8187±0.0153	0.8490±0.0138	0.8553±0.0110	0.8276±0.0244	0.8252±0.0297
	L.	0.7669±0.0083	0.7573±0.0099	0.8762±0.0116	0.8687±0.0099	0.8359±0.0087	0.8267±0.0175	0.8470±0.0068	0.8460±0.0087	0.8315±0.0463	0.8247±0.0481
	S.+L.	0.7506±0.0093	0.7433±0.0127	0.7838±0.0289	0.8013±0.0129	0.8580±0.0011	0.8560±0.0020	0.8452±0.0099	0.8493±0.0046	0.8094±0.0509	0.8125±0.0521
votek	S.+E.	0.8281±0.0060	0.8133±0.0050	0.8193±0.0045	0.8127±0.0070	0.8199±0.0103	0.8113±0.0136	0.8602±0.0074	0.8520±0.0104	0.8319±0.0193	0.8223±0.0198
	S.+E.+L.	0.7473±0.0118	0.7467±0.0130	0.8659±0.0076	0.8600±0.0035	0.8146±0.0211	0.7913±0.0291	0.8447±0.0155	0.8420±0.0223	0.8181±0.0517	0.8100±0.0513
NeuronPattern	Neuron	0.8346±0.0097	0.8320±0.0122	0.7918±0.0224	0.7707±0.0181	0.8595±0.0121	0.8507±0.0155	0.8400±0.0122	0.8506±0.0123	0.8341±0.0301	0.8233±0.0359
Llama-3.2-3B-Instruct											
Method	#Shot	5		10		20		30		Avg.	
	InfoType	Macro-F1	Acc	Macro-F1	Acc	Macro-F1	Acc	Macro-F1	Acc	Macro-F1	Acc
Random	N/A	0.6374±0.0066	0.6460±0.0080	0.7095±0.0197	0.7207±0.0046	0.7265±0.0284	0.6960±0.0111	0.7203±0.0167	0.7633±0.0153	0.6985±0.0413	0.7065±0.0490
Patron	S.+E.	0.6884±0.0098	0.7107±0.0083	0.6839±0.0066	0.7320±0.0053	0.7899±0.0107	0.7787±0.0170	0.7472±0.0161	0.7727±0.0101	0.7273±0.0507	0.7485±0.0326
Entropy	Highest	0.6892±0.0055	0.6673±0.0042	0.6709±0.0146	0.6453±0.0153	0.6520±0.0229	0.6413±0.0050	0.6384±0.0048	0.5967±0.0070	0.6626±0.0222	0.6377±0.0296
	Diverse	0.7645±0.0086	0.7467±0.0064	0.7888±0.0152	0.7813±0.0133	0.7028±0.0166	0.7687±0.0070	0.6884±0.0363	0.7380±0.0193	0.7361±0.0482	0.7587±0.0199
TypiClust	S.	0.7392±0.0226	0.7327±0.0208	0.7398±0.0083	0.7320±0.0060	0.6829±0.0300	0.7107±0.0186	0.8030±0.0236	0.8007±0.0136	0.7412±0.0491	0.7440±0.0391
	L.	0.7457±0.0064	0.7413±0.0070	0.6794±0.0104	0.6427±0.0133	0.7278±0.0082	0.7833±0.0133	0.6964±0.0746	0.7940±0.0111	0.7123±0.0300	0.7403±0.0690
	S.+L.	0.6918±0.0159	0.6793±0.0121	0.7647±0.0148	0.7867±0.0058	0.7728±0.0256	0.7573±0.0127	0.7843±0.0206	0.7780±0.0140	0.7534±0.0418	0.7503±0.0489
fast-votek	S.	0.7386±0.0185	0.7567±0.0150	0.7966±0.0111	0.8033±0.0163	0.7455±0.0235	0.7327±0.0172	0.7603±0.0254	0.7520±0.0260	0.7602±0.0259	0.7612±0.0300
	L.	0.6910±0.0044	0.6820±0.0080	0.7826±0.0059	0.7780±0.0080	0.7019±0.0121	0.7340±0.0250	0.6947±0.0215	0.7627±0.0201	0.7176±0.0436	0.7392±0.0422
	S.+L.	0.7755±0.0095	0.7873±0.0110	0.7138±0.0265	0.7647±0.0064	0.6976±0.0350	0.7567±0.0205	0.7184±0.0319	0.7927±0.0190	0.7263±0.0340	0.7753±0.0174
votek	S.+E.	0.7520±0.0031	0.7587±0.0129	0.7517±0.0107	0.7453±0.0167	0.8012±0.0219	0.7867±0.0181	0.7165±0.0108	0.7940±0.0131	0.7554±0.0348	0.7712±0.0230
	S.+E.+L.	0.7576±0.0163	0.7607±0.0136	0.7845±0.0034	0.7793±0.0095	0.7233±0.0312	0.7567±0.0117	0.7629±0.0363	0.8087±0.0095	0.7571±0.0254	0.7763±0.0237
NeuronPattern	Neuron	0.7335±0.0072	0.7147±0.0050	0.7193±0.0199	0.7587±0.0092	0.7845±0.0259	0.8207±0.0147	0.7781±0.0117	0.7493±0.0117	0.7538±0.0323	0.7608±0.0442

Table 9: Experimental results with Llama series on TREC.

Method	#Shot	5		10		20		30		Avg.	
	InfoType	Macro-F1	Acc	Macro-F1	Acc	Macro-F1	Acc	Macro-F1	Acc	Macro-F1	Acc
Qwen3-8B											
Random	N/A	0.2980±0.0301	0.2798±0.0247	0.4128±0.0070	0.3864±0.0080	0.4448±0.0043	0.4216±0.0056	0.4726±0.0031	0.4646±0.0051	0.4071±0.0767	0.3881±0.0790
Patron	S.+E.	0.3373±0.0236	0.3128±0.0210	0.4406±0.0058	0.4170±0.0065	0.4634±0.0065	0.4459±0.0091	0.4906±0.0027	0.4867±0.0042	0.4330±0.0670	0.4156±0.0743
Entropy	Highest	0.2748±0.0283	0.2621±0.0212	0.4231±0.0126	0.3990±0.0149	0.4509±0.0047	0.4332±0.0065	0.4853±0.0035	0.4827±0.0053	0.4085±0.0927	0.3943±0.0946
	Diverse	0.3355±0.0201	0.3093±0.0179	0.4005±0.0124	0.3724±0.0125	0.4477±0.0042	0.4260±0.0055	0.4725±0.0035	0.4611±0.0063	0.4141±0.0603	0.3922±0.0662
TypiClust	S.	0.2980±0.0277	0.2790±0.0220	0.4201±0.0082	0.3951±0.0095	0.4613±0.0040	0.4437±0.0060	0.4800±0.0034	0.4726±0.0066	0.4149±0.0818	0.3976±0.0853
	L.	0.3135±0.0292	0.2923±0.0244	0.3860±0.0142	0.3578±0.0154	0.4449±0.0039	0.4225±0.0043	0.4688±0.0024	0.4542±0.0040	0.4033±0.0692	0.3817±0.0719
	S.+L.	0.2813±0.0242	0.2656±0.0190	0.4039±0.0142	0.3758±0.0151	0.4480±0.0041	0.4266±0.0050	0.4763±0.0024	0.4658±0.0044	0.4024±0.0861	0.3834±0.0868
FastVoteK	S.	0.2475±0.0262	0.2420±0.0185	0.3876±0.0153	0.3615±0.0150	0.4551±0.0044	0.4362±0.0062	0.4823±0.0039	0.4767±0.0059	0.3931±0.1049	0.3791±0.1031
	L.	0.2762±0.0326	0.2629±0.0258	0.3758±0.0164	0.3485±0.0153	0.4335±0.0055	0.4092±0.0062	0.4787±0.0046	0.4709±0.0064	0.3911±0.0874	0.3729±0.0887
	S.+L.	0.3327±0.0255	0.3091±0.0222	0.4099±0.0124	0.3823±0.0135	0.4531±0.0034	0.4332±0.0043	0.4883±0.0023	0.4847±0.0038	0.4210±0.0670	0.4024±0.0749
VoteK	S.+E.	0.3452±0.0191	0.3189±0.0175	0.3754±0.0139	0.3481±0.0135	0.4534±0.0028	0.4320±0.0039	0.4716±0.0057	0.4632±0.0081	0.4114±0.0607	0.3905±0.0682
	S.+E.+L.	0.3335±0.0251	0.3098±0.0220	0.4092±0.0128	0.3819±0.0137	0.4528±0.0032	0.4331±0.0044	0.4880±0.0031	0.4844±0.0044	0.4209±0.0666	0.4023±0.0745
NeuronPattern	Neuron	0.3611±0.0253	0.3341±0.0232	0.4166±0.0102	0.3911±0.0117	0.4706±0.0035	0.4593±0.0054	0.4886±0.0023	0.4866±0.0036	0.4342±0.0575	0.4178±0.0687
Qwen3-4B-Instruct-2507											
Method	#Shot	5		10		20		30		Avg.	
	InfoType	Macro-F1	Acc	Macro-F1	Acc	Macro-F1	Acc	Macro-F1	Acc	Macro-F1	Acc
Random	N/A	0.4242±0.0144	0.4102±0.0211	0.4252±0.0017	0.4154±0.0038	0.4384±0.0069	0.4284±0.0093	0.4135±0.0070	0.3922±0.0094	0.4253±0.0102	0.4115±0.0150
Patron	S.+E.	0.4089±0.0147	0.3929±0.0203	0.4422±0.0034	0.4382±0.0054	0.4199±0.0115	0.4033±0.0158	0.3557±0.0186	0.3301±0.0179	0.4067±0.0367	0.3911±0.0451
Entropy	Highest	0.4195±0.0198	0.4039±0.0273	0.4488±0.0093	0.4443±0.0121	0.4280±0.0097	0.4153±0.0126	0.4580±0.0038	0.4542±0.0041	0.4386±0.0179	0.4295±0.0237
	Diverse	0.4431±0.0094	0.4374±0.0135	0.4150±0.0085	0.3987±0.0121	0.4326±0.0076	0.4201±0.0117	0.4194±0.0112	0.3990±0.0148	0.4275±0.0128	0.4138±0.0187
TypiClust	S.	0.4325±0.0111	0.4252±0.0170	0.4474±0.0067	0.4434±0.0086	0.4594±0.0013	0.4565±0.0018	0.4350±0.0092	0.4231±0.0124	0.4436±0.0124	0.4371±0.0158
	L.	0.4079±0.0081	0.3887±0.0119	0.4099±0.0062	0.3930±0.0079	0.4063±0.0038	0.3863±0.0055	0.3649±0.0237	0.3372±0.0231	0.3973±0.0216	0.3763±0.0262
	S.+L.	0.4096±0.0118	0.3934±0.0171	0.3883±0.0118	0.3626±0.0133	0.4210±0.0077	0.4069±0.0097	0.4369±0.0127	0.4284±0.0160	0.4140±0.0204	0.3978±0.0275
FastVoteK	S.	0.3990±0.0098	0.3775±0.0129	0.4229±0.0047	0.4109±0.0065	0.4054±0.0099	0.3842±0.0139	0.3980±0.0109	0.3730±0.0132	0.4063±0.0115	0.3864±0.0170
	L.	0.3862±0.0239	0.3633±0.0263	0.4328±0.0133	0.4245±0.0186	0.4221±0.0095	0.4096±0.0120	0.4218±0.0102	0.4058±0.0135	0.4157±0.0203	0.4008±0.0263
	S.+L.	0.4265±0.0164	0.4148±0.0232	0.4179±0.0074	0.4037±0.0115	0.4401±0.0033	0.4346±0.0065	0.4373±0.0085	0.4270±0.0122	0.4304±0.0102	0.4200±0.0136
VoteK	S.+E.	0.4148±0.0093	0.4010±0.0144	0.4132±0.0056	0.4013±0.0071	0.4252±0.0079	0.4154±0.0106	0.4078±0.0123	0.3860±0.0146	0.4153±0.0073	0.4009±0.0120
	S.+E.+L.	0.3886±0.0388	0.3693±0.0445	0.3816±0.0314	0.3579±0.0348	0.4061±0.0048	0.3846±0.0076	0.4050±0.0090	0.3823±0.0116	0.3953±0.0121	0.3735±0.0124
NeuronPattern	Neuron	0.4566±0.0025	0.4550±0.0024	0.4454±0.0010	0.4389±0.0007	0.4540±0.0014	0.4495±0.0009	0.4645±0.0010	0.4625±0.0021	0.4551±0.0079	0.4515±0.0099

Table 10: Experimental results with Qwen3 series on MMLU-Pro.

Qwen3-8B											
Method	#Shot	5		10		20		30		Avg.	
	InfoType	Macro-F1	Acc	Macro-F1	Acc	Macro-F1	Acc	Macro-F1	Acc	Macro-F1	Acc
Random	N/A	0.5097±0.0015	0.5103±0.0014	0.5779±0.0016	0.5788±0.0017	0.6691±0.0007	0.6970±0.0014	0.6898±0.0013	0.7122±0.0020	0.6116±0.0836	0.6246±0.0967
Patron	S.+E.	0.6753±0.0004	0.7265±0.0007	0.6391±0.0016	0.7363±0.0004	0.6421±0.0012	0.6550±0.0017	0.6809±0.0009	0.7180±0.0017	0.6593±0.0218	0.7089±0.0367
Entropy	Highest	0.5057±0.0016	0.5065±0.0015	0.5273±0.0019	0.5274±0.0019	0.5726±0.0019	0.5732±0.0020	0.6158±0.0019	0.6205±0.0022	0.5554±0.0490	0.5569±0.0507
	Diverse	0.6022±0.0019	0.6077±0.0022	0.6009±0.0017	0.6053±0.0020	0.6561±0.0004	0.6913±0.0017	0.6668±0.0018	0.7484±0.0003	0.6315±0.0349	0.6632±0.0695
TypiClust	S.	0.4488±0.0017	0.4540±0.0015	0.6329±0.0016	0.6432±0.0020	0.6587±0.0014	0.6855±0.0023	0.6778±0.0008	0.7324±0.0009	0.6045±0.1055	0.6288±0.1221
	L.	0.6460±0.0016	0.6574±0.0019	0.6065±0.0016	0.6119±0.0018	0.6027±0.0032	0.6075±0.0036	0.6501±0.0014	0.6725±0.0024	0.6263±0.0252	0.6373±0.0325
	S.+L.	0.4683±0.0019	0.4717±0.0017	0.5688±0.0018	0.5695±0.0019	0.6466±0.0010	0.6655±0.0017	0.6701±0.0011	0.6934±0.0018	0.5885±0.0911	0.6000±0.1006
FastVoteK	S.	0.6011±0.0013	0.6083±0.0016	0.6460±0.0009	0.6723±0.0015	0.6660±0.0004	0.6983±0.0008	0.6454±0.0016	0.6669±0.0024	0.6396±0.0274	0.6615±0.0380
	L.	0.5339±0.0021	0.5346±0.0023	0.6383±0.0023	0.6526±0.0028	0.6612±0.0012	0.6787±0.0018	0.6489±0.0023	0.6622±0.0029	0.6206±0.0585	0.6320±0.0658
	S.+L.	0.4712±0.0020	0.4742±0.0018	0.6555±0.0014	0.6826±0.0021	0.6421±0.0026	0.6519±0.0031	0.6879±0.0005	0.7150±0.0012	0.6142±0.0972	0.6310±0.1076
VoteK	S.+E.	0.6456±0.0009	0.6729±0.0016	0.6651±0.0006	0.6973±0.0012	0.6685±0.0007	0.7127±0.0013	0.6945±0.0011	0.7210±0.0020	0.6684±0.0201	0.7010±0.0211
	S.+E.+L.	0.6401±0.0008	0.6607±0.0012	0.6717±0.0002	0.7085±0.0010	0.6107±0.0011	0.6188±0.0016	0.6008±0.0026	0.6035±0.0028	0.6308±0.0320	0.6479±0.0471
NeuronPattern	Neuron	0.6679±0.0001	0.7088±0.0009	0.6680±0.0010	0.6928±0.0014	0.6724±0.0005	0.7033±0.0012	0.6424±0.0023	0.7378±0.0004	0.6627±0.0137	0.7107±0.0193
Qwen3-4B-Instruct-2507											
Method	#Shot	5		10		20		30		Avg.	
	InfoType	Macro-F1	Acc	Macro-F1	Acc	Macro-F1	Acc	Macro-F1	Acc	Macro-F1	Acc
Random	N/A	0.5612±0.0016	0.5612±0.0017	0.6119±0.0027	0.6145±0.0029	0.7115±0.0008	0.7382±0.0013	0.7283±0.0009	0.7528±0.0015	0.6532±0.0800	0.6667±0.0937
Patron	S.+E.	0.7022±0.0011	0.7660±0.0003	0.6624±0.0014	0.7554±0.0003	0.6616±0.0008	0.6980±0.0016	0.7142±0.0004	0.7487±0.0013	0.6851±0.0271	0.7420±0.0302
Entropy	Highest	0.4661±0.0023	0.4712±0.0021	0.5513±0.0019	0.5513±0.0019	0.5849±0.0023	0.5855±0.0024	0.6178±0.0016	0.6208±0.0018	0.5550±0.0652	0.5572±0.0640
	Diverse	0.6596±0.0018	0.6675±0.0021	0.5964±0.0017	0.5978±0.0018	0.7141±0.0017	0.7344±0.0026	0.7151±0.0014	0.7371±0.0018	0.6713±0.0563	0.6842±0.0660
TypiClust	S.	0.5132±0.0018	0.5133±0.0018	0.5820±0.0032	0.5831±0.0034	0.6955±0.0015	0.7149±0.0022	0.7129±0.0006	0.7486±0.0014	0.6259±0.0949	0.6400±0.1106
	L.	0.6381±0.0015	0.6433±0.0017	0.6535±0.0012	0.6614±0.0014	0.6163±0.0034	0.6193±0.0037	0.6373±0.0022	0.6441±0.0026	0.6363±0.0153	0.6420±0.0173
	S.+L.	0.5047±0.0013	0.5055±0.0012	0.5915±0.0023	0.5937±0.0024	0.6528±0.0024	0.6656±0.0029	0.7037±0.0017	0.7283±0.0024	0.6132±0.0856	0.6233±0.0958
FastVoteK	S.	0.6307±0.0021	0.6366±0.0024	0.6824±0.0008	0.7187±0.0003	0.6921±0.0009	0.7367±0.0009	0.6885±0.0006	0.7345±0.0013	0.6734±0.0287	0.7066±0.0474
	L.	0.5935±0.0015	0.5321±0.0013	0.6769±0.0008	0.7126±0.0024	0.6901±0.0013	0.7006±0.0017	0.6861±0.0006	0.7474±0.0012	0.6617±0.0457	0.6732±0.0961
	S.+L.	0.5321±0.0013	0.5991±0.0018	0.6903±0.0018	0.6967±0.0012	0.6847±0.0011	0.7138±0.0017	0.7124±0.0003	0.7072±0.0011	0.6549±0.0827	0.6792±0.0539
VoteK	S.+E.	0.6003±0.0013	0.6022±0.0014	0.6658±0.0009	0.6797±0.0011	0.6943±0.0012	0.7203±0.0017	0.6934±0.0009	0.7224±0.0017	0.6635±0.0442	0.6812±0.0562
	S.+E.+L.	0.6023±0.0012	0.6059±0.0013	0.6874±0.0006	0.7092±0.0011	0.7131±0.0007	0.7363±0.0011	0.7225±0.0003	0.7575±0.0006	0.6813±0.0548	0.7022±0.0672
NeuronPattern	Neuron	0.7081±0.0002	0.7651±0.0002	0.7097±0.0004	0.7353±0.0006	0.6659±0.0009	0.6747±0.0011	0.6833±0.0001	0.7248±0.0008	0.6918±0.0211	0.7250±0.0376

Table 11: Experimental results with Qwen3 series on Edu-Feedback.

Qwen3-8B											
Method	#Shot	5		10		20		30		Avg.	
	InfoType	Macro-F1	Acc	Macro-F1	Acc	Macro-F1	Acc	Macro-F1	Acc	Macro-F1	Acc
Random	N/A	0.8295±0.0023	0.8207±0.0031	0.8246±0.0071	0.7947±0.0095	0.8467±0.0004	0.8113±0.0012	0.8737±0.0027	0.8640±0.0040	0.8436±0.0222	0.8227±0.0296
Patron	S.+E.	0.8189±0.0030	0.8213±0.0031	0.7989±0.0082	0.8160±0.0072	0.8259±0.0048	0.8093±0.0070	0.8543±0.0017	0.8473±0.0031	0.8245±0.0230	0.8235±0.0166
Entropy	Highest	0.8069±0.0099	0.8167±0.0042	0.8194±0.0013	0.8220±0.0020	0.8356±0.0045	0.8327±0.0061	0.8861±0.0037	0.8847±0.0042	0.8370±0.0348	0.8390±0.0312
	Diverse	0.8532±0.0019	0.8473±0.0012	0.8579±0.0053	0.8413±0.0031	0.8699±0.0057	0.8567±0.0023	0.8410±0.0004	0.8180±0.0020	0.8555±0.0119	0.8408±0.0165
TypiClust	S.	0.8003±0.0044	0.7980±0.0069	0.8282±0.0038	0.8240±0.0035	0.8507±0.0029	0.8460±0.0020	0.8436±0.0071	0.8433±0.0031	0.8307±0.0223	0.8278±0.0222
	L.	0.8212±0.0033	0.8353±0.0012	0.7995±0.0058	0.7673±0.0070	0.8570±0.0023	0.8493±0.0023	0.8637±0.0006	0.8527±0.0012	0.8354±0.0303	0.8262±0.0399
	S.+L.	0.8413±0.0035	0.8333±0.0050	0.8467±0.0058	0.8380±0.0053	0.8562±0.0038	0.8287±0.0050	0.8588±0.0054	0.8400±0.0000	0.8508±0.0082	0.8350±0.0051
FastVoteK	S.	0.8461±0.0047	0.8413±0.0064	0.8571±0.0012	0.8420±0.0020	0.8172±0.0051	0.7993±0.0070	0.8411±0.0005	0.8393±0.0012	0.8404±0.0168	0.8305±0.0208
	L.	0.8416±0.0011	0.8420±0.0020	0.8587±0.0051	0.8533±0.0012	0.8773±0.0006	0.8567±0.0012	0.8384±0.0021	0.8193±0.0050	0.8540±0.0179	0.8428±0.0169
	S.+L.	0.8314±0.0018	0.8427±0.0012	0.8661±0.0030	0.8653±0.0012	0.8642±0.0024	0.8473±0.0023	0.8836±0.0028	0.8593±0.0023	0.8613±0.0218	0.8537±0.0105
VoteK	S.+E.	0.8392±0.0044	0.8307±0.0058	0.8411±0.0033	0.8320±0.0035	0.8458±0.0013	0.8387±0.0012	0.8309±0.0049	0.8527±0.0050	0.8393±0.0062	0.8385±0.0101
	S.+E.+L.	0.8441±0.0016	0.8433±0.0023	0.8438±0.0008	0.8460±0.0000	0.8374±0.0032	0.8080±0.0035	0.8309±0.0027	0.8053±0.0061	0.8391±0.0062	0.8257±0.0220
NeuronPattern	Neuron	0.8237±0.0040	0.8287±0.0031	0.8654±0.0009	0.8727±0.0012	0.8856±0.0015	0.8600±0.0020	0.8717±0.0056	0.8687±0.0023	0.8616±0.0266	0.8575±0.0199
Qwen3-4B-Instruct-2507											
Method	#Shot	5		10		20		30		Avg.	
	InfoType	Macro-F1	Acc	Macro-F1	Acc	Macro-F1	Acc	Macro-F1	Acc	Macro-F1	Acc
Random	N/A	0.8039±0.0016	0.8047±0.0012	0.8754±0.0009	0.8713±0.0012	0.8848±0.0013	0.8820±0.0020	0.8698±0.0029	0.8813±0.0031	0.8585±0.0369	0.8598±0.0371
Patron	S.+E.	0.8193±0.0015	0.8267±0.0012	0.8258±0.0039	0.8387±0.0012	0.8646±0.0021	0.8773±0.0031	0.8598±0.0048	0.8673±0.0012	0.8424±0.0231	0.8525±0.0238
Entropy	Highest	0.8405±0.0019	0.8393±0.0023	0.8521±0.0035	0.8540±0.0035	0.8592±0.0044	0.8620±0.0040	0.8681±0.0035	0.8713±0.0031	0.8550±0.0116	0.8567±0.0136
	Diverse	0.8363±0.0015	0.8473±0.0023	0.8613±0.0012	0.8753±0.0012	0.8712±0.0024	0.8707±0.0023	0.8807±0.0010	0.8753±0.0012	0.8624±0.0191	0.8672±0.0134
TypiClust	S.	0.8344±0.0014	0.8633±0.0031	0.8558±0.0036	0.8667±0.0031	0.8688±0.0024	0.8653±0.0012	0.8509±0.0083	0.8693±0.0023	0.8525±0.0142	0.8662±0.0025
	L.	0.8696±0.0008	0.8707±0.0012	0.8655±0.0062	0.8553±0.0023	0.8615±0.0015	0.8680±0.0020	0.8504±0.0060	0.8580±0.0020	0.8618±0.0083	0.8630±0.0075
	S.+L.	0.8341±0.0035	0.8467±0.0012	0.8428±0.0009	0.8507±0.0012	0.8732±0.0008	0.8607±0.0012	0.8704±0.0009	0.8753±0.0012	0.8551±0.0196	0.8583±0.0128
FastVoteK	S.	0.8677±0.0029	0.8660±0.0035	0.8690±0.0011	0.8687±0.0012	0.8656±0.0007	0.8653±0.0012	0.8878±0.0028	0.8827±0.0031	0.8725±0.0103	0.8707±0.0081
	L.	0.8260±0.0000	0.8520±0.0000	0.8556±0.0010	0.8533±0.0012	0.8743±0.0015	0.8780±0.0020	0.8882±0.0017	0.8847±0.0023	0.8610±0.0269	0.8670±0.0168
	S.+L.	0.8151±0.0049	0.8213±0.0023	0.8559±0.0005	0.8607±0.0012	0.8777±0.0004	0.8807±0.0012	0.8402±0.0013	0.8633±0.0012	0.8472±0.0263	0.8565±0.0251
VoteK	S.+E.	0.8442±0.0040	0.8380±0.0053	0.8515±0.0000	0.8480±0.0000	0.8551±0.0001	0.8660±0.0000	0.8608±0.0007	0.8487±0.0012	0.8529±0.0069	0.8502±0.0116
	S.+E.+L.	0.8002±0.0043	0.8180±0.0020	0.8747±0.0035	0.8747±0.0012	0.8587±0.0061	0.8473±0.0023	0.8804±0.0032	0.8453±0.0046	0.8535±0.0367	0.8463±0.0231
NeuronPattern	Neuron	0.8390±0.0025	0.8613±0.0012	0.8624±0.0022	0.8713±0.0031	0.8771±0.0000	0.8860±0.0000	0.8800±0.0038	0.8947±0.0042	0.8646±0.0188	0.8783±0.0149

Table 12: Experimental results with Qwen3 series on TREC.

Nora Belrose, Zach Furman, Logan Smith, Danny Halawi, Igor Ostrovsky, Lev McKinney, Stella Biderman, and Jacob Steinhardt. 2023. Eliciting latent predictions from transformers with the tuned lens. *arXiv preprint arXiv:2303.08112*.

Tom Brown, Benjamin Mann, Nick Ryder, Melanie Subbiah, Jared D Kaplan, Prafulla Dhariwal, Arvind Neelakantan, Pranav Shyam, Girish Sastry, Amanda Askell, and 1 others. 2020. Language models are few-shot learners. *Advances in neural information processing systems*, 33:1877–1901.

Yixin Cao, Jiahao Ying, Yaoning Wang, Xipeng Qiu, Xuanjing Huang, and Yugang Jiang. 2025. Model utility law: Evaluating llms beyond performance through mechanism interpretable metric. *Preprint*, arXiv:2504.07440.

Kang Chen, Yaoning Wang, Kai Xiong, Zhuoka Feng, Wenhe Sun, Haotian Chen, and Yixin Cao. 2025. Do llms signal when they're right? evidence from neuron agreement. *arXiv preprint arXiv:2510.26277*.

David Cohn, Zoubin Ghahramani, and Michael Jordan. 1994. Active learning with statistical models. *Advances in neural information processing systems*, 7.

Yarin Gal, Riashat Islam, and Zoubin Ghahramani. 2017. Deep bayesian active learning with image data. In *International conference on machine learning*, pages 1183–1192. PMLR.

Leo Gao, Tom Dupré la Tour, Henk Tillman, Gabriel Goh, Rajan Troll, Alec Radford, Ilya Sutskever, Jan Leike, and Jeffrey Wu. 2024. Scaling and evaluating sparse autoencoders. *arXiv preprint arXiv:2406.04093*.

Tianyu Gao, Xingcheng Yao, and Danqi Chen. 2021. SimCSE: Simple contrastive learning of sentence embeddings. In *Proceedings of the 2021 Conference on Empirical Methods in Natural Language Processing*, pages 6894–6910, Online and Punta Cana, Dominican Republic. Association for Computational Linguistics.

Mor Geva, Roei Schuster, Jonathan Berant, and Omer Levy. 2021. Transformer feed-forward layers are key-value memories. In *Proceedings of the 2021 Conference on Empirical Methods in Natural Language Processing*, pages 5484–5495, Online and Punta Cana, Dominican Republic. Association for Computational Linguistics.

Aaron Grattafiori, Abhimanyu Dubey, Abhinav Jauhri, Abhinav Pandey, Abhishek Kadian, Ahmad Al-Dahle, Aiesha Letman, Akhil Mathur, Alan Schelten, Alex Vaughan, and 1 others. 2024. The llama 3 herd of models. *arXiv preprint arXiv:2407.21783*.

Jiaxin Guo, CL Philip Chen, Shuzhen Li, and Tong Zhang. 2024. Deuce: Dual-diversity enhancement and uncertainty-awareness for cold-start active learning. *Transactions of the Association for Computational Linguistics*, 12:1736–1754.

Guy Hacohen, Avihu Dekel, and Daphna Weinshall. 2022. Active learning on a budget: Opposite strategies suit high and low budgets. In *International Conference on Machine Learning*, pages 8175–8195. PMLR.

SU Hongjin, Jungo Kasai, Chen Henry Wu, Weijia Shi, Tianlu Wang, Jiayi Xin, Rui Zhang, Mari Ostendorf, Luke Zettlemoyer, Noah A Smith, and 1 others. 2022. Selective annotation makes language models better few-shot learners. In *The Eleventh International Conference on Learning Representations*.

Lei Huang, Weijiang Yu, Weitao Ma, Weihong Zhong, Zhangyin Feng, Haotian Wang, Qianglong Chen, Weihua Peng, Xiaocheng Feng, Bing Qin, and 1 others. 2025. A survey on hallucination in large language models: Principles, taxonomy, challenges, and open questions. *ACM Transactions on Information Systems*, 43(2):1–55.

Jaehun Jung, Seungju Han, Ximing Lu, Skyler Hallinan, David Acuna, Shrimai Prabhumoye, Mostafa Patwary, Mohammad Shoeybi, Bryan Catanzaro, and Yejin Choi. 2025. Prismatic synthesis: Gradient-based data diversification boosts generalization in llm reasoning. *arXiv preprint arXiv:2505.20161*.

Leonard Kaufman. 1990. Partitioning around medoids (program pam). *Wiley series in probability and statistics*, 344:68–125.

Lorenz Kuhn, Yarin Gal, and Sebastian Farquhar. 2023. Semantic uncertainty: Linguistic invariances for uncertainty estimation in natural language generation. *arXiv preprint arXiv:2302.09664*.

Woosuk Kwon, Zhuohan Li, Siyuan Zhuang, Ying Sheng, Lianmin Zheng, Cody Hao Yu, Joseph Gonzalez, Hao Zhang, and Ion Stoica. 2023. Efficient memory management for large language model serving with pagedattention. In *Proceedings of the 29th symposium on operating systems principles*, pages 611–626.

Xin Li and Dan Roth. 2002. Learning question classifiers. In *COLING 2002: The 19th International Conference on Computational Linguistics*.

William C Mann and Sandra A Thompson. 1988. Rhetorical structure theory: Toward a functional theory of text organization. *Text-interdisciplinary Journal for the Study of Discourse*, 8(3):243–281.

Katerina Margatina, Timo Schick, Nikolaos Aletras, and Jane Dwivedi-Yu. 2023. Active learning principles for in-context learning with large language models. In *Findings of the Association for Computational Linguistics: EMNLP 2023*, pages 5011–5034.

Yu Meng, Jiaming Shen, Chao Zhang, and Jiawei Han. 2019. Weakly-supervised hierarchical text classification. In *Proceedings of the AAAI conference on artificial intelligence*, volume 33, pages 6826–6833.

Sewon Min, Xinxi Lyu, Ari Holtzman, Mikel Artetxe, Mike Lewis, Hannaneh Hajishirzi, and Luke Zettlemoyer. 2022. Rethinking the role of demonstrations: What makes in-context learning work? In *Proceedings of the 2022 Conference on Empirical Methods in Natural Language Processing*, pages 11048–11064.

Nostalgebraist. 2020. Interpreting GPT: The logit lens. https://www.lesswrong.com/posts/AcCRPn5w6xmtPRD7j/interpreting-gpt-the-logit-lens. LessWrong.

Christopher Schröder, Andreas Niekler, and Martin Potthast. 2021. Revisiting uncertainty-based query strategies for active learning with transformers. *arXiv preprint arXiv:2107.05687*.

Yubo Wang, Xueguang Ma, Ge Zhang, Yuansheng Ni, Abhranil Chandra, Shiguang Guo, Weiming Ren, Aaran Arulraj, Xuan He, Ziyan Jiang, and 1 others. 2024. Mmlu-pro: A more robust and challenging multi-task language understanding benchmark. *arXiv preprint arXiv:2406.01574*.

Yong Wu and Christian D Schunn. 2023. Passive, active, and constructive engagement with peer feedback: A revised model of learning from peer feedback. *Contemporary Educational Psychology*, 73:102160.

Yu Xia, Subhojyoti Mukherjee, Zhouhang Xie, Junda Wu, Xintong Li, Ryan Aponte, Hanjia Lyu, Joe Barrow, Hongjie Chen, Franck Dernoncourt, and 1 others. 2025. From selection to generation: A survey of llm-based active learning. *arXiv preprint arXiv:2502.11767*.

An Yang, Anfeng Li, Baosong Yang, Beichen Zhang, Binyuan Hui, Bo Zheng, Bowen Yu, Chang Gao, Chengen Huang, Chenxu Lv, and 1 others. 2025. Qwen3 technical report. *arXiv preprint arXiv:2505.09388*.

Guoxin Yu, Lemao Liu, Haiyun Jiang, Shuming Shi, and Xiang Ao. 2023a. Retrieval-augmented few-shot text classification. In *Findings of the Association for Computational Linguistics: EMNLP 2023*, pages 6721–6735, Singapore. Association for Computational Linguistics.

Yue Yu, Rongzhi Zhang, Ran Xu, Jieyu Zhang, Jiaming Shen, and Chao Zhang. 2023b. Cold-start data selection for better few-shot language model fine-tuning: A prompt-based uncertainty propagation approach. In *Proceedings of the 61st Annual Meeting of the Association for Computational Linguistics (Volume 1: Long Papers)*, pages 2499–2521.

Michelle Yuan, Hsuan-Tien Lin, and Jordan Boyd-Graber. 2020. Cold-start active learning through self-supervised language modeling. *arXiv preprint arXiv:2010.09535*.